國 立 交 通 大 學

電子物理學系

碩士論文

經由微波退火形成極薄且均勻厚度的鎳矽
化物研究

A study of Ultrathin and Homogenous Ni
Silicide Formed by Low Temperature
Microwave Annealing

指導教授：趙天生 博士

研 究 生：謝其儒

中 華 民 國 一 ○ ○ 年 七 月

經由微波退火形成極薄且均勻厚度的鎳矽化物研究

A study of Ultrathin and Homogenous Ni Silicide Formed by Low Temperature Microwave Annealing

研究生: 謝其儒   **Student: Chi-Ju Hsieh**

指導教授: 趙天生   **Advisor: Tien-Sheng Chao**

國立交通大學 電子物理學系

碩士論文

A Thesis

Submitted to Department of Electrophysics

National Chiao Tung University

In Partial Fulfillment of the Requirements

for the Degree of Master of Science

In Electrophysics

June 2011

Hsinchu, Taiwan, Republic of China

中 華 民 國 一 ○○ 年 六 月

經由微波退火形成極薄且均勻厚度的鎳矽化物研究

國立交通大學電子物理所

指導教授：趙天生 博士　　　　　　　　　　　　　研究生：謝其儒

摘要

　　近來，國際半導體科技走勢圖(ITRS)對金屬矽化物的厚度預估已達到下修瓶頸，故本論文主要探討在室溫下以物理氣相沉積 15 奈米(nm)的鎳金屬在矽基板上，再以低溫微波形成金屬矽化物層(Ni Silicide layer)，進而採用兩段式退火方式形成擁有低片電阻值、極薄且均勻厚度的鎳矽化物，以提前符合 2012-2021 的半導體架構需求。第一階段的退火是利用低功率的微波退火進行，它會促進鎳金屬擴散進入矽基板中。接著在去除未反應的金屬後，再進行第二次的微波退火，藉此以降低片電阻和晶相的轉換。此外，在微波腔體內分別以不同的擺放方式和數量置入石英片和矽晶片，亦會得到不同厚度、阻值和晶相的鎳矽化物，其機制將會在本篇論文裡詳細闡述。第二次退火透過最佳化的擺設方式和功率調整，我們所形成的鎳矽化物的厚度僅從 9 奈米增加到 10.5 奈米，而其片電阻值從 170 歐姆/□降至 18 歐姆/□。

　　除此之外，我們也在矽基板上透過超高真空化學氣相沉積方式磊晶一層約 200 奈米的純鍺，之後運用以上的技術做出一層鎳鍺化物(Ni Germanide layer)，其特性亦會在本論文中詳細描述。

　　另外，我們也將此微波退火的技術整合在九十奈米的場效電晶體元件的製程上，其汲極電流和漏電流都因此獲得顯著的改善。

A study of Ultrathin and Homogenous Ni Silicide Formed by Low Temperature Microwave Annealing

Department of Electrophysics,

National Chiao Tung University

Advisor: Dr. Tien-Sheng, Chao   **Student: Chi Ju, Hsieh**

Abstract

For the recent years, ITRS has encountered bottlenecks for predicting the downscaled thickness of nickel silicide (NiSi); therefore in this thesis, we investigated low temperature formation of Ni Silicide layer by physical chemical deposition(PVD) in room temoerature of a 15nm Ni layer on (100) Si substrate.. The formation of ultrathin, homogenoues and low sheet resistance (Rs) Ni silicide film was formed by two-step annealing in order to meet the specifications of 2012-2021 single and multi-gate MPU/ASIC required by ITRS 2010. The first step is applying the low power microwave annealing, which promotes Ni diffusion through a thin interfacial amorphous layer. Then the unreacted metal will be lifted off after first step is finished. The second step annealing is applied in order to lower sheet resistance and firmly merge the phase. Furthermore, inserting quartz and Si suscpetors upon/below the primary wafer with different setups and quantities will also result in different thickness, Rs and phase. Its mechanism will be detailed in this thesis as well. The optimized 2nd step MWA is the key to reduce the Ni-silicide sheet resistance to a record low 18 ohm/sq. from 170 ohm/square (ohm/sq.) while Ni silicide thickness is just slightly increased from 9 nm to 10.5 nm.

In addition, we deposited a 2000~3000nm Germanium (Ge) layer upon (100) Si substrate by ultrahigh vacuum chemical vapor deposition (UHVCVD) in order to form the nickel germanide (NiGe) through aforementioned process techniques. Its characteristics will be further discussed in this thesis as well.

Besides, we have microwave annealing integrated into 90nm Metal Oxide Semiconductor Field Effect Transistors (MOSFETs) fabrication process. The drain current and leakage are both improved by this novel annealing techniques.

誌謝

Acknowledgements

岷臻學姊、林威良學長、莊尚勳學長、薛富國學長等；也謝謝與我同時期進入這大家庭的夥伴：紡織少東添舜、作實驗時默念你名字總讓我如有神助的芳昌、氣質正妹立盈、心思細膩的昱璇、天兵一號聖文、Tetris 一哥哲維、ITO 一哥其驊、老歌唱匠育豪、iMac 星瑋，有你們的陪伴讓生活充滿歡笑；最後謝謝學弟妹:剛正不阿的勁軒、情義相挺歡樂送的柔含、明慈以及夏國譯讓實驗室變得更加活潑、我們出遊的歡樂笑聲亦將永遠回盪在心頭。在各自追逐夢想之際，感謝也祝福大家未來能順利通過各個階段的考驗。

感謝國家奈米實驗室的全體員工在實驗上給予我的協助，其中謝謝工程師姚潔宜小姐、彭馨誼小姐、林昆霖先生、宋柏融先生，以及代工小姐:綉芝姐、鳳姐、庭瑋姐、家如姐、子綾姐、李姐、婉貞姐總是在實驗中給予我許多的方便。

最後，我要對我的父親謝秉叡先生、母親彭秀蘭女士和姊姊謝涵君致上最深的謝意，感謝你們總是提供一個最好的環境、最舒服的家，讓我有一個心靈的避風港，你們對我不辭辛勞的照顧、栽培以及鼓勵是我背後最大的原動力，因此我把畢業的榮耀與你們一起分享。

我要特別感謝在碩士班最辛苦的時候一路陪伴我的余子于小姐，謝謝妳的不離不棄，以及妳對我的包容，感謝妳為我付出的一切。

同時，我謹以這篇論文獻給所有在碩士班其間給予我幫助以及關懷的人，謝謝你們。

Contents

Figure Caption

Chapter 1

Chapter 2

Chapter 3

Table Caption

Chapter 1

Chapter 2

Chapter 3

Chapter 1

Introduction

1.1   Origin of silicide

Complementary metal-oxide-semiconductor (CMOS) has become the predominant technology in very large-scale integrated (VLSI) circuits due to its many advantages such as higher performance, lower power consumption, and higher operation speed and device density. As the ongoing evolution of CMOS, the scaling of integrated circuits has promoted the operation speed and the density of CMOS circuits; however, the resistances of source, drain and gate will be dramatically increased with the downscaled device dimension. Therefore, the self-aligned silicide (salicide) technique is presented to reduce the series resistance of a device [1.1] [1.2].

Since the resistance between source and drain is formulated in the composition of contact resistance (R_{co}), source drain extension resistance (R_{SDE}), spreading resistance (R_{sp}), accumulation resistance (R_{ac}) and sheet resistance (Rs) as shown in Equ. 1. Therefore, plenty of techniques are developed to reduce the above resistances such as lightly doped drain (LDD) and source drain extension.

$$R_{sd} = R_{co} + R_{SDE} + R_{sp} + R_{ac} + R_{sh} \text{ ……………. Equ. 1}$$

Now we concentrate on reducing sheet resistance and contact resistance. Their magnitudes vary from different materials applied. Therefore, discreet selection of materials for silicide is a very important issue, and it also activates the further researches of silicide in the following 30 years.

1.2   Evolution of polyicide

Nickel, as now wildly regarded as metal material, is not the first one applied to

react with silicon to form silicide. In this section, the evolution of silicide will be revealed in detail. At first, it was tungsten (W), tantalum (Ta) and molybdenum (Mo), which reacted with silicon to form so-called "polycide (stacked silicide/poly-Si gate electrode)". In the species of polycide as shown in Fig. 1-1, the $MoSi_2$ polycide was the first introduced to LSI fabrication in the early 1980s; and then followed by WSi_2, which was popularly applied due to its lower sheet resistance rather than $MoSi_2$. However, in polycide case, silicide film peeling-off during thermal process due to the different expansion coefficients of the two layers, which became a serious issue to worry. Furthermore, the implanted dopants diffused into silicide resulted in increased sheet resistance and the shifts of threshold voltage (Vt) [1.1].

1.3   Evolution of salicide

For above reasons stated in section 1.2, IC engineers developed new techniques to substitute polycide – "self-aligned silicide (salicide)" as the device scaling down towards 100nm. Titanium was the first species to react with silicon to form titanium salicide ($TiSi_2$), and the reason was attributed to its low resistivity and lower sheet resistance than WSi_2; nonetheless, there are two major issues concerning $TiSi_2$.

The first issue is the huge contact resistance. When $TiSi_2$ was applied in the p-type region, $TiSi_2$ layer will absorb huge numbers of boron (B) atoms to form the P^+ silicon layer during the thermal process. In other words, Ti tends to react with implanted dopants such as boron and arsenic to form the bonding of Ti-B and Ti-As instead of Ti-Si [1.3] [1.4]. Thus, the barrier height for electrons and holes at $TiSi_2$-Si contact area increased as stated in Table 1-2. In addition, Ti may also form a bridge between the gate and source/drain region by silicidation due to the main diffusion species of titanium silicide is Si. This effect is named "Bridge effect", and its

2

mechanism will be detailed later in the section 1.4.2.

The other issue concerning $TiSi_2$ is its dual phase - C49 and C54. C49 has higher resistivity (60-70 μΩ-cm), which can be transformed into lower resistivity by high temperature (>800°C) thermal process. However, incomplete transformation from C49 to C54 may occur in deep submicron integration due to the thinner line width or thickness and relatively larger grain size, which will result in the lack of nucleation center in nanoscale transistors. Besides, silicon molecular is the main diffusion species as aforementioned and less metal near edge could react with silicon during the silicidation. These factors lead to thinner thickness of silicide and increased sheet resistance consequently.

For such reasons, IC engineers came up with new species – Co to replace Ti. Both Ti and Co have good thermal stability. But unlike $TiSi_2$, the superiorities of $CoSi_2$ are less thin film stress and even better stability; furthermore, $CoSi_2$ would not react with implanted dopants. The less thin film stress is improved by excellent lattice constant with silicon (about 12%). Major drawback of Co silicide is its silicon consumption issue. (Co : Si : $CoSi_2$ = 1 nm: 3.63 nm: 3.49 nm) [1.3].

Followed by Co, Ni is extensively applied in the material of silicide in current nanoscale transistors; therefore, Ni silicide is the primary object to discuss in this thesis. There are three main phases of Ni silicide, which are di-nickel silicide (Ni_2Si), nickel mono-silicide (NiSi) and nickel di-silicide ($NiSi_2$) respectively. The following essay will briefly explain the characteristics of these three Ni silicides mentioned above. The Ni_2Si, with relatively higher resistivity, is formed by annealing temperature from 150°C to 300°C for Ni and silicon substrate. Besides, its phase gets unstable for temperature above 300°C and transforms into Ni mono-silicide (NiSi) phase. The NiSi is more thermally stable, and its resistivity is the lowest

(14~20 μΩ-cm) among three different phases and other metal silicides such as Co silicides, Ti silicides and polycides [1.5]. Furthermore, less silicon consumption, wilder annealing temperature window (as shown in Fig 1-2) [1.6] [1.7], and lower barrier height for holes (as stated in Table 1-2) catch the great research popularity and build its success in metal silicides [1.8] [1.9].

NiSi$_2$, usually being identified in pyramids shapes, is transformed by NiSi followed by higher temperature. The agglomeration phenomenon is observed with grain boundary grooving and inhomogeneous surface energy absorbance, which will result in the formation of silicide islands ultimately [1.10]. The sheet resistance will then rise dramatically [1.11] [1.12].

1.4   Phenomenon during the silicidation

Here we are about to discuss the phenomenon such as silicon consumption issue , bridge effect, narrow line width effect which concern us during the silicidation.

1.4.1   Silicon consumption issue

The range of silicon consumption for silicide is defined as the distance normalized by silicide thickness, and the distance is that between the initial surfaces of silicon to bottom of silicide. The silicon consumption issue is an important ingredient for forming ultra-shallow junction (USJ) for sub-100 nm node CMOS. Table 1-1 indicates how many (nm) of Si per nm metal is required for resultant silicide thickness, and we are able to notice that for the Si consumption of NiSi is less than CoSi$_2$ and TiSi$_2$. However, the requirements are also varied from different phase in NiSi as detailed in Fig. 1-3 [1.13].

1.4.2 Bridge effect

The bridging effect takes place when silicide formed on the gate sidewall, which results in short circuit area between gate and source/drain. The reason of bridge effect could be attributed to the primary moving species of the silicide. There are two different conditions during silicidation at the sidewall as shown in Fig. 1-4. The bridging effect would occur if the primary moving species is Si. Take titanium silicide for instance, silicon atoms of $TiSi_2$ diffuses into the titanium film including the sidewall area during silicidation which lead to bridging failure. The resistivity of the silicide and its primary moving species are also indicated in Table 1-3.

1.4.3 Narrow line width effect

In the process of forming silicide, the edge of the silicide will be less reacted if the silicon is the primary moving species. The thickness of the silicide thus gets thinner and results in sheet resistance increasing as shown in Fig. 1-5.

1.5 Motivation

Since we have reviewed the history of the silicide, we are acknowledged that the evolution is on its way to both lower the sheet/contact resistance and thinner thickness during the downscaled CMOS fabrication. In section 1.5.1, current technique of forming the silicide in summary is presented in summary. In section 1.5.2, we will examine the specification of ITRS 2010 for Ni silicides in the future.

In the current development of Ni silicide, it has encountered the barriers of its evolution toward both lowering the thickness and phase issue. In this thesis, we will provide the solutions for this bottleneck – Microwave annealing (MWA).

1.5.1   Necessity of downscaled silicide thickness in USJ

As the downscaling in gate length of transistors, the concept of ultra shallow junction (USJ) is proposed to prevent the punch-through and drain induced barrier lowering (DIBL), which will result in catastrophic performance. However, thicker silicide thickness would probably overstride the dopant region then contact with the Si substrate, which leads to great leakage. Therefore reducing the silicide thickness in USJ becomes a critical issue to solve.

1.5.2   Summary table for current techniques

Table 1-3 [1.14] ~ [1.17] summarizes the comparison of recently reported Ni silicidation techniques. It is worthwhile to note that two-step MWA achieves record combination of low sheet resistance of 18 ohm/sq. and silicide thickness of 10.5 nm.

1.5.3   Specification for ITRS

According to ITRS 2010 [1.18], ultrathin (< 11 nm) silicide contacts in the source/drain region are required for 2012-2021 MPU/ASIC as shown in Fig. 1-6. NiSi currently faces difficult trade-offs between thickness and sheet resistance. In this work, a novel two-step MWA process is used to form homogeneous NiSi contact films with low sheet resistance while not sacrificing thickness and quality. This technique is promising for achieving 15 nm-node CMOS and beyond. Use of MWA provides a NiSi thickness (10.5 nm), 40% thinner than previously reported silicide results.
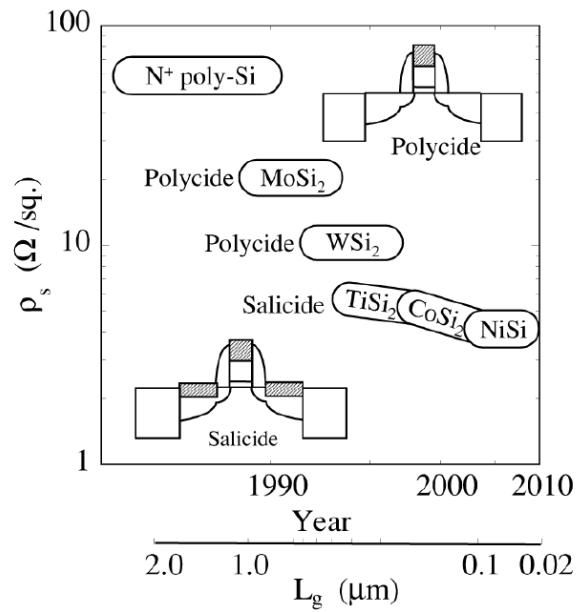
Fig. 1- 1   Evolution history of silicide materials, which implies NiSi is extensively applied from 2000s [1.1].

(a)
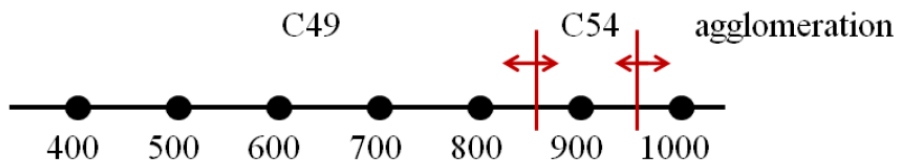
(b)
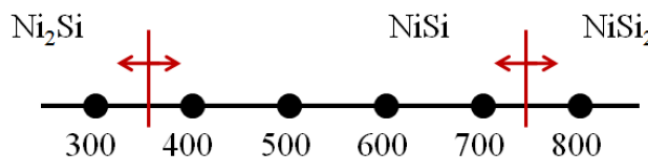
Fig. 1- 2   The phase of silicide in different annealing temperatures: (a) Ti silicide, (b) Ni silicide.
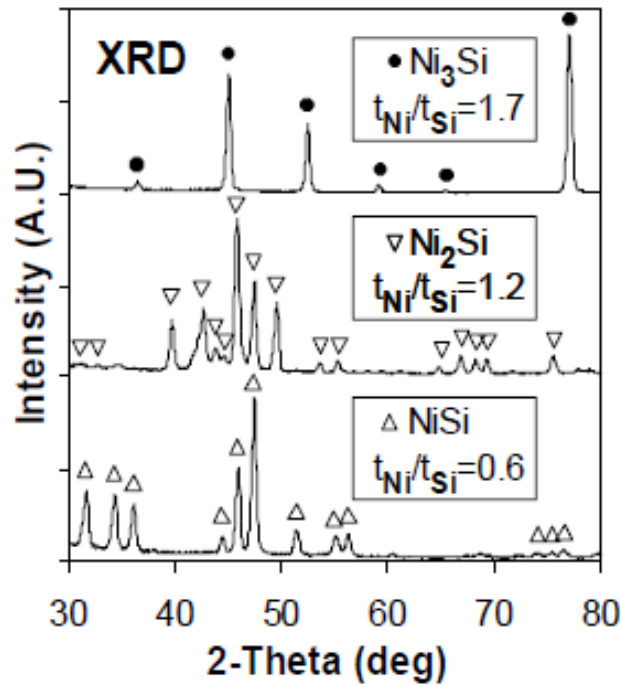
Fig. 1- 3 XRD spectra identifies the formation of Ni₃Si, NiSi and Ni₂Si by adjusting

Ni to Si thickness ratio, which indicates the formation of NiSi requires less Ni. [1.13]
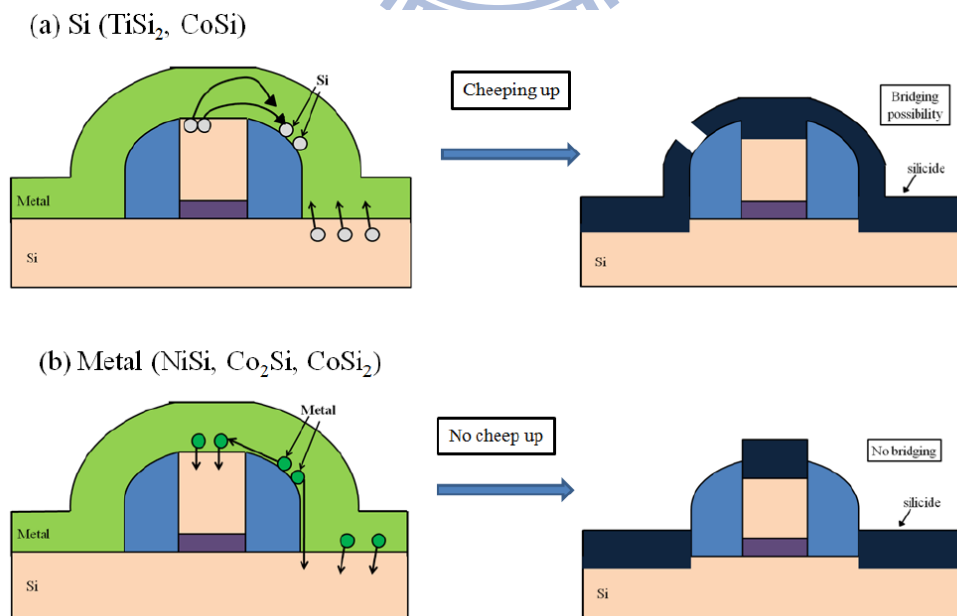
Fig. 1- 4 Moving species at the gate sidewall during silicidation [1.1].
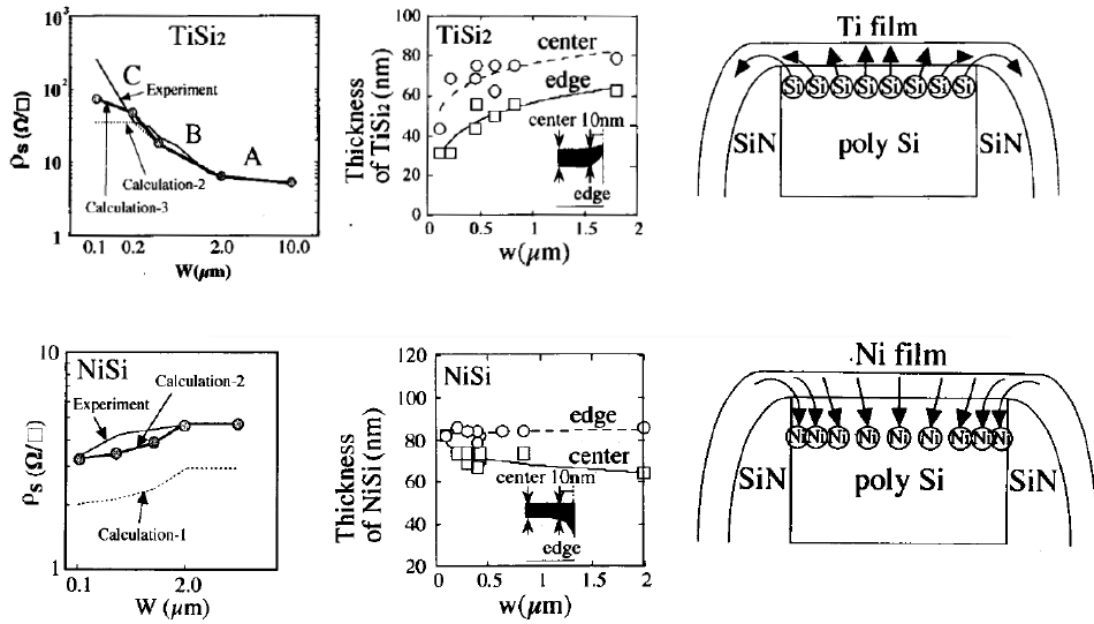
Fig. 1- 5   The mechanism of narrow line width effect in Ti silicide and Ni silicide
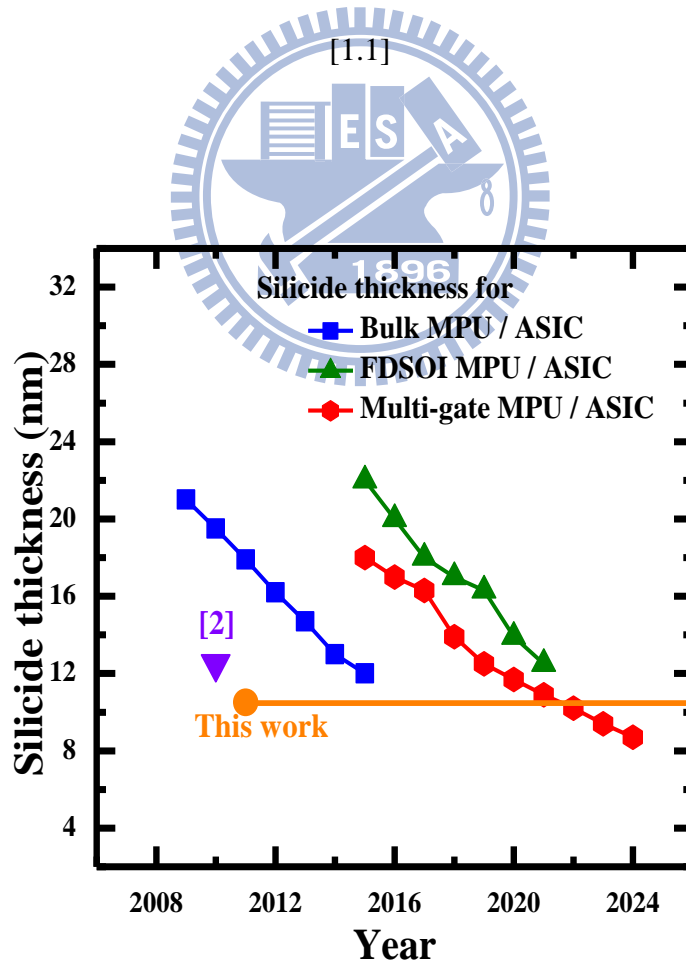
Fig. 1- 6   Silicide thickness requirement by ITRS 2010 [1.18]

Silicide	Resistivity	Stable on Si up to (^{o}C)	nm of Si consumed per nm of metal	nm of resulting silicide per nm of metal	Barrier height to n-Si (eV)
MoSi$_2$	40-100	~1000	2.56	2.59	0.64
WSi$_2$	30-70	~1000	2.53	2.58	0.67
TiSi$_2$(C54)	13-16	~900	2.27	2.51	0.58
TiSi$_2$(C49)	60-70	N/A	2.27	2.51	N/A
Co$_2$Si	~70	N/A	0.91	1.47	N/A
CoSi	100-150	N/A	1.82	2.02	N/A
CoSi$_2$	14-20	~950	3.64	3.52	0.65
NiSi	14-20	~650	1.67	2.34	N/A
NiSi$_2$	40-50	N/A	3.65	3.63	0.66

Table 1- 1   Some properties of metal silicides.
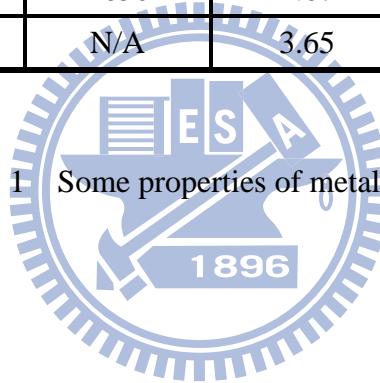
Silicide	Barrier height for electron(eV)	Barrier height for holes (eV)
NiSi	0.67	0.43
CoSi	0.65	0.45
TiSi$_2$	0.61	0.49
MoSi$_2$	0.56	0.54

Table 1- 2   Schottky barrier heights of various silicides.

Silicide	Resistivity (μΩ-cm)	Moving species
TiSi$_2$	10-15	Si
CoSi$_2$	18	Co
CoSi	>180	Si
Co$_2$Si	>180	Co
NiSi	20	Ni
PtSi	28-35	Pt
Pd$_2$Si	30-35	Pd, Si
WSi$_2$	70	Si
MoSi$_2$	100	Si

Table 1- 3　Silicide with its resistivity corresponding to its primary moving species.

Reference		This thesis	[1.14]	[1.15] [1.16]	[1.17]	[1.17]
Tools of thermal process		MWA	MWA	SLA	Soak RTA	Spike RTA
Steps of thermal process		2	N/A	1	2	2
Temp. (^{o}C)/ Duration (sec)	1st step	140/300	250	250/(N/A)	200/30	220/(Negligible)
	2nd step	360/300	N/A	N/A	400/30	400(Negligible)
Ni/Ti(N) (nm)		15/15	N/A	6 nm NiPt	10/10	10/10
Phase of Ni(Pt) silicide		NiSi	NiPtSi	NiPtSi	NiSi	NiSi
Silicide thickness (nm)		10.5	12.5	17	~10	Unmentioned
Sheet resistance (ohm/sq.)		18	N/A	25	34	40

Table 1- 4　Summarizes the comparison of recently reported Ni silicidation

techniques.

Chapter 2

Device Fabrication and Experimental Setup

2.1 Introduction

Inasmuch as the microwave becomes a promising solution for solving the resistance – thickness dilemma, the characteristics of microwave annealing (MWA) and the process flow for both of blanket NiSi layer formed by MWA and RTA on Si substrate, 90 nm pMOSFET fabrications and blanket NiGe layer will be detailed in this chapter.

2.2 Microwave mechanism

This section primarily discusses the mechanism of microwave as title, which will be divided into two parts: characteristics of microwave and electromagnetic phenomenon observed in microwave annealing.

2.2.1 Characteristics of microwave

The microwave is regarded as one of the electromagnetic waves, and its wavelength is between the 1 m and 1 mm with corresponding frequency from 0.3 GHz to 300 GHz. The frequency of microwave is usually applied in 800 MHz, 2.45 GHz, 5.8 GHz, and 13 GHz in commercial or experimental use. Here the frequency of microwave in this study was applied in 5.8 GHz.

Microwave annealing has attracted much attention in dopant activation due to its unique features such as low temperature, non-ionizing and harmlessness to internal

structure [2.1] [2.2]. In this thesis, NiSi with record a combination of low thickness and resistance is achieved by inserting quartz and Si susceptors above and below process wafers during MWA. With different thermal budgets and setups as identified in Fig. 2-1, MWA leads to various silicide sheet resistance, thickness and phase. The maximum wafer surface temperatures at power levels of 360W, 600W and 1300W are 170 ^{o}C, 260 ^{o}C and 360 ^{o}C as shown in Fig. 2-2. The temperature is detected through the hole which located in the center of Si susceptors by pyrometer, as shown in Fig. 2-3. The absorption of microwave power by quartz wafers is negligible. Quartz placed near the process wafer remains lower temperature and can cool the process wafer. In contrast, Si susceptors placed near the process wafer help to heat it. Setup 1 thus produces a lower wafer temperature than setup 2.

2.2.2 Electromagnetic phenomenon in microwave annealing

In traditional concepts, thicker silicide thickness by RTA comes with thicker metal layer deposited. However, opposite results will be observed if MWA is applied due to its unique electromagnetic property – skin depth [2.3] [2.4]. The reciprocal of skin depth is attenuation constant (α). Numerical data as stated in Table 2-1, attenuation constants varied from different materials can be calculated by electromagnetic theory where μ stands for permeability and σ stands for conductivity. If we assume certain thickness of metal layer, such as 15nm for Ni, the decay of microwave is thus able to be extracted by the formula. After calculation, loss of 0.3% intensity, 9% intensity and 21% intensity will be lost when microwave penetrating Ti layer of 15nm, Ni layer of 15nm and slightly boron doped Si of 695 μm respectively. The skin depth (implies 36.7% intensity remained) is 175 nm and 4340 nm for Ti layer of 15nm and Ni layer of 15nm respectively, which are

13

reasonable for the intensity decay calculated above. More intensity loss occurs with less metal reacts when microwave penetrates into thicker metal layer, which implies opposite results against traditional concepts.

A simple experiment is demonstrated to support our theoretical hypothesis. As shown in Fig. 2-4 in contrast to RTA, thicker Ni film deposited results in higher sheet resistance than thinner Ni film due to attenuation mechanism of microwave power through the Ni/Ti layers.

2.3　Device fabrication

2.3.1　The ultrathin blanket Ni silicide film formed by only MWA

The blanket Ni Silicide refers itself formed by blanket Ni deposited on the bare-Si wafer without any patterns. All samples were prepared on the silicon wafer with boron-doped P-type with (100)-orientation. First, the silicon wafers were dipped in a 100:1 diluted HF (DHF) solution to remove the native oxide after the standard clean (STD clean), and then rinsed with DI water followed by spin dry. In order to remove the particles, metal ions and organics, the STD clean procedure is applied by rinsing SC-1(NH_4OH：H_2O_2：$H_2O \rightarrow 0.25$：1：5) and SC-2(HCl：H_2O_2：$H_2O \rightarrow 1$：1：6), each for 10mins. Then the wafers were rinsed with DI water for a short time to prevent the native oxide. After the STD clean and HF dip, the 15 nm Ni film and 15 nm Ti film were deposited on silicon substrates after ion clean process (ICP) clean to remove the native oxide in physical vapor deposition (PVD) as shown in Fig 2-5(a). Then the sample would be first annealed by microwave with 360W in setup 1and setup 2 for 300 sec, as shown in Fig. 2-5(b). After the first stage annealing, the unreacted nickel film and titanium film were selectively etched using the H_2SO_4:H_2O_2

14

(3:1) solution at 120 ^{o}C, as shown in Fig.2-6(c). The second step of annealing was applied by different microwave power: 600W in setup 2 for 300sec and 1300W in setup 2 for 300sec.

2.3.2 The blanket Ni silicide film formed by RTA and MWA

After the cleaning procedure which is simply the same as aforementioned technique, the 15 nm Ni film and 15 nm Ti film were deposited on silicon substrates after ion clean process (ICP) clean to remove the native oxide in physical vapor deposition (PVD) as shown in Fig 2-6(a). Then the sample would be first annealed by RTA 180°C and 260°C for 15 sec, as shown in Fig. 2-6(b). After the first stage annealing, the unreacted nickel film and titanium film were selectively etched using the H$_2$SO$_4$:H$_2$O$_2$ (3:1) solution at 120 ^{o}C, as shown in Fig.2-6(c). The second step of annealing was applied by different annealing methods: RTA 450°C for 15sec and MWA 1300W in setup 2 for 300sec.

2.3.3 The integration of 90 nm pMOSFET Device

After the cleaning procedure which is the same as aforementioned technique, the Local Oxidation of Silicon (LOCOS) isolation for devices is implemented. Then 2.5nm gate oxide and 120nm un-doped poly gate were deposited and patterned in 90 nm line width. Followed by pocket, extension ion implant, and then spacer was formed and etched. After source and drain ion implant is implemented by BF$_2$ with dosage of 5E15, spike annealing takes place for activation. The 15 nm Ni film and 15 nm Ti film were deposited on silicon substrates after ion clean process (ICP) clean to remove the native oxide in physical vapor deposition (PVD), then devices would be first annealed by microwave with 360W in setup 2 for 300 sec. After the first stage

annealing, the unreacted nickel film and titanium film were selectively etched using the $H_2SO_4:H_2O_2$ (3:1) solution at 120 ^{o}C. The second step of annealing was applied by MWA 1300W in setup 2 as shown in Fig. 2-6 and Fig. 2-7. The control split in order to compare is the device without NiSi formation.

2.3.4 The blanket Ni germanide film formation

After the cleaning procedure which is the same as aforementioned technique, we deposited a 2000~3000nm germanium (Ge) layer upon (100) Si substrate by ultrahigh vacuum chemical vapor deposition (UHVCVD). Then 15 nm Ni/15 nm Ti and 25nm Ni/15nm Ti were deposited on bare-Si (100) substrates respectively after ion clean process (ICP) clean to remove the native oxide in physical vapor deposition (PVD). Then the sample would be first annealed by MWA with 360W in setup 1 compared with RTA in 350°C, 450°C, 550°C and 650°C respectively, as shown in Fig. 2-8.

2.4 Measurements and analysis

The four-point probe was used to measure the sheet resistance of Ni silicide film which determined the phase transition and agglomeration of silicide. The phase of silicide was determined by the X-ray diffraction (XRD) and Selected Area Diffraction Pattern (SADP). Fig. 2-9 shows the connection of each measurement apparatus for I-V curve and leakage characteristics which is composed of semiconductor characterization system (KEITHLEY 4200), two channel pulse generator (Agilent 81110A), low leakage current switch mainframe (KEITHLEY 708A) and the probe station. Stable measuring environments provide us accurate electrical characteristics extraction. The cross-sectional morphologies of silicide were inspected by Transmission Electron Microcopy (TEM) to check the thickness of silicide.
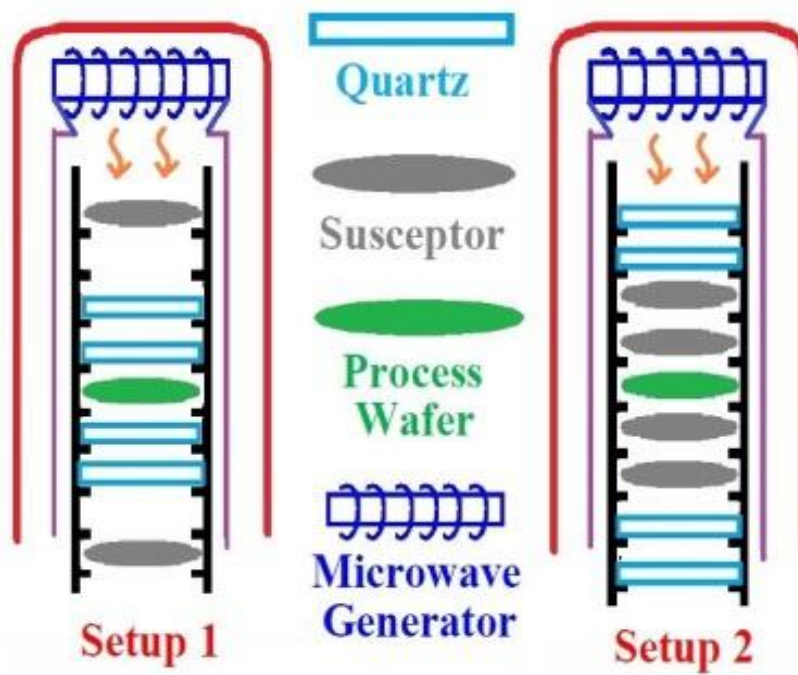
Fig. 2- 1　Schematic illustration of the MWA system. Quartz and Si susceptors inside

chamber change the absorption efficiency of the process wafer. Different setups result

in different peak temperature during microwave annealing.
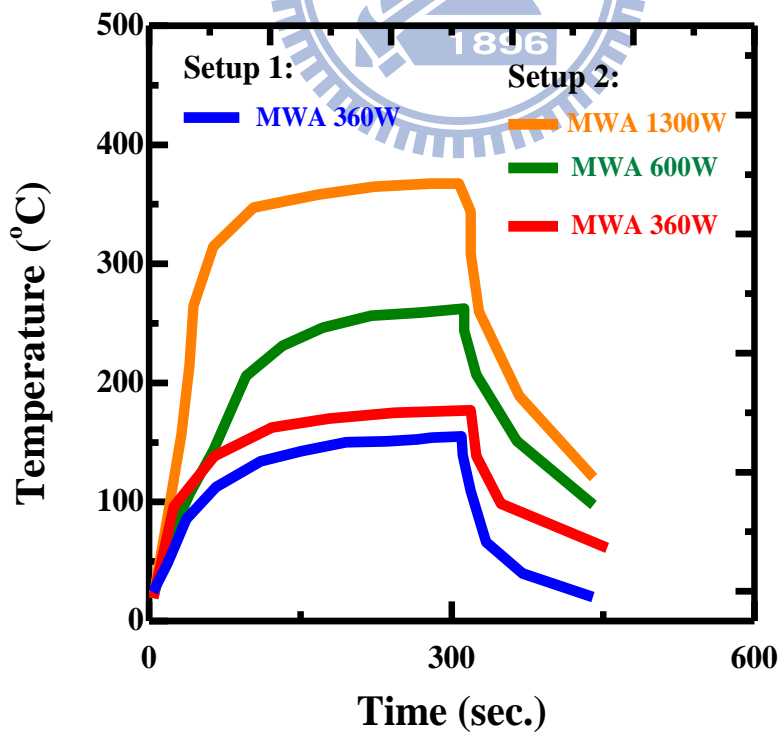
Fig. 2- 2　The temperature profiles at different power levels measured with a

pyrometer. Temperature increased with more power applied

17
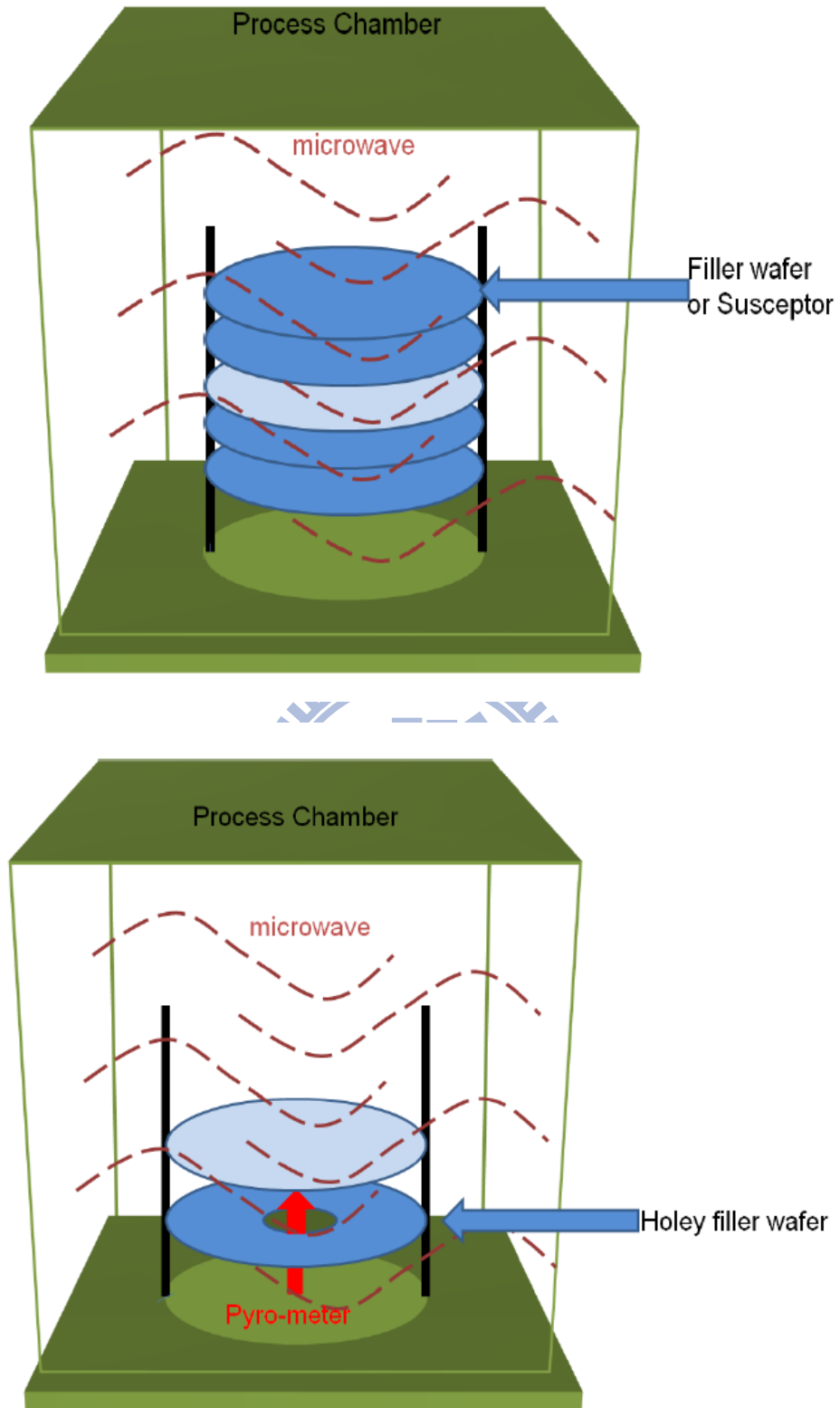
Fig. 2- 3   The schematic figure of microwave chamber, infrared rays detect the temperature of process wafer through the hole located in the center of wafers.
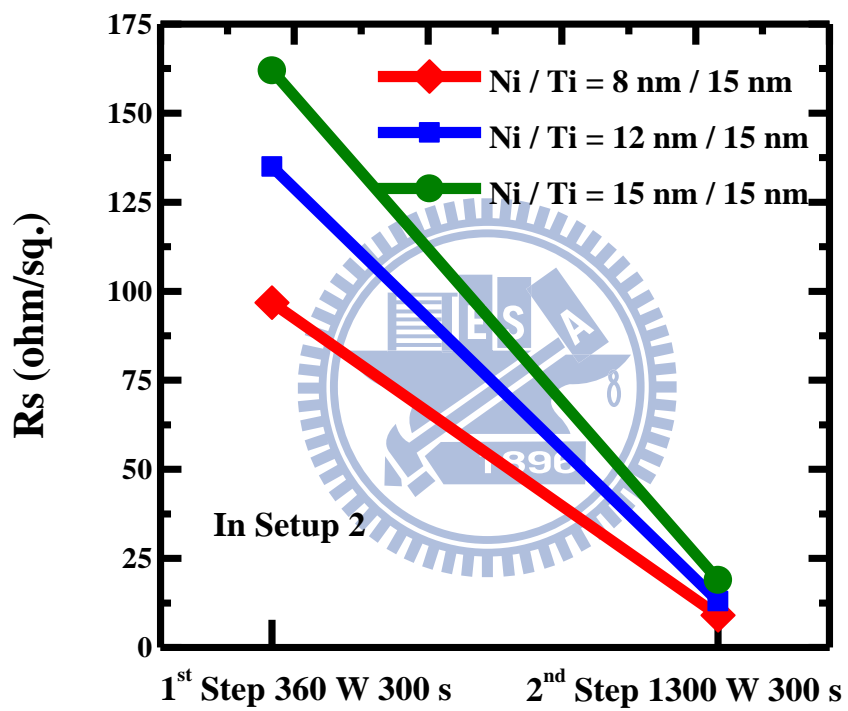
Fig. 2- 4   Thicker Ni films results in higher Rs due to attenuation of microwave power through the Ni/Ti layers. Thicker metal layer deposited results in more power dissipated, which implies thinner silicide will be formed.
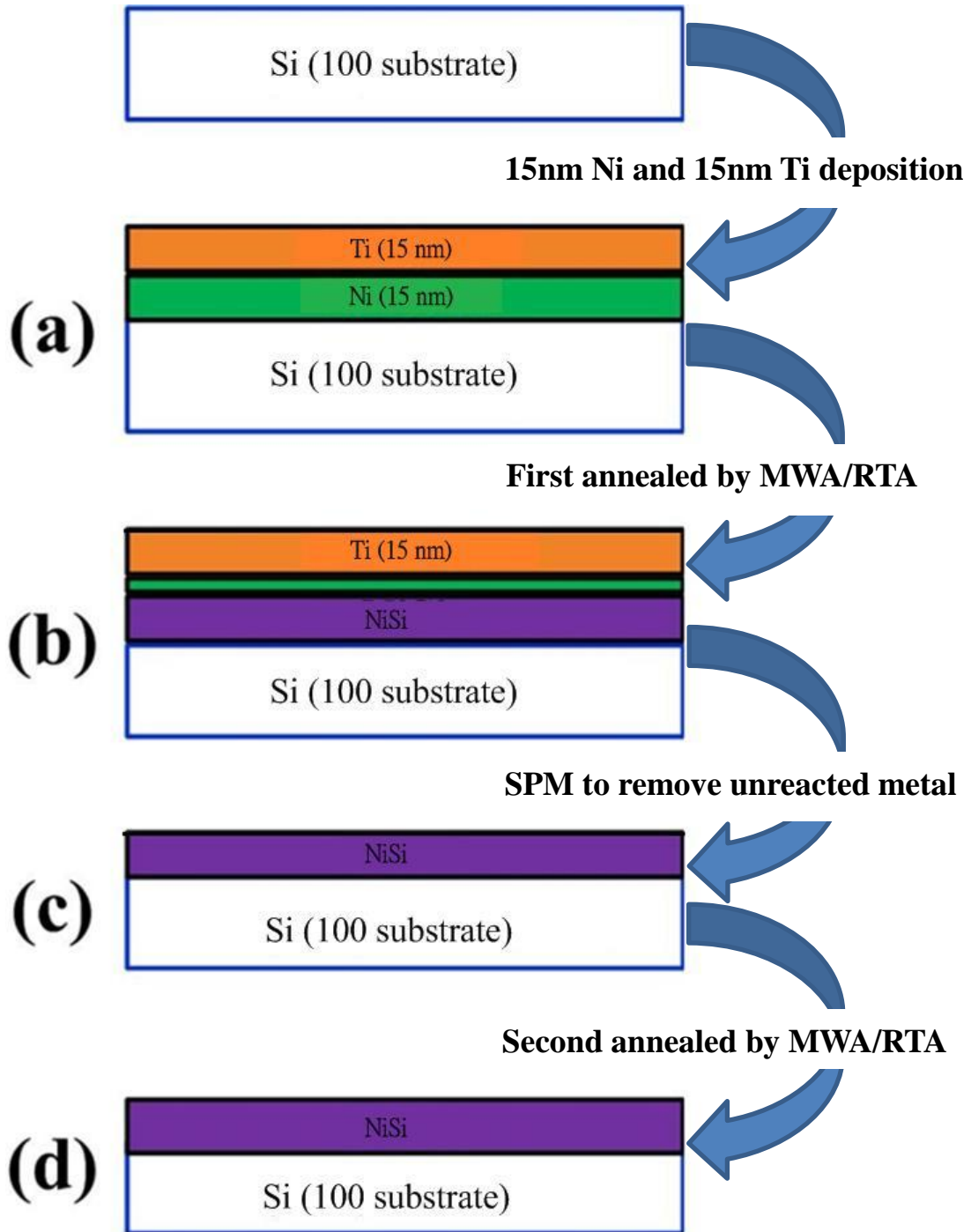
Fig. 2- 5 The process flow of the sample of Ni-silicide on Si substrate.

Device isolation

Gate stack deposition and patterned

Pocket & Extension Ion Implant

Spacer formation

S/D Ion Implantation

Spike annealing

Ni/Ti = 15/15 (nm) deposition

1st step: MWA

Silicidation

2nd step anneal: MWA

Fig. 2- 6   The process flow of 90 nm pMOSFET fabrication
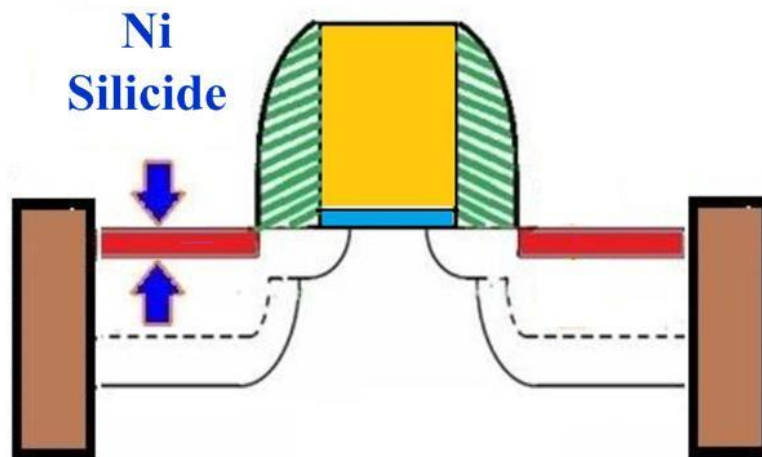
Fig. 2- 7   The figure of 90 nm pMOSFET device, and Ni silicide is formed in the

source-drain area.

Si (100) substrate

2000 nm germanium layer deposited by UHVCVD

(a)

Ge (2000 nm)

Si (100) substrate

15 nm Ni/15 nm Ti and 25 nm Ni/ 15nm Ti were deposited by PVD

(b)

Ti (15 nm)

Ni (15 nm)

Ge (2000 nm)

Si (100) substrate

First annealed by Microwave in 360W for 300sec / RTA

(c)

Ti (15 nm)

NiGe

Si (100) substrate

Fig. 2- 8 The process flow of the sample of Ni germanide on Si substrate.
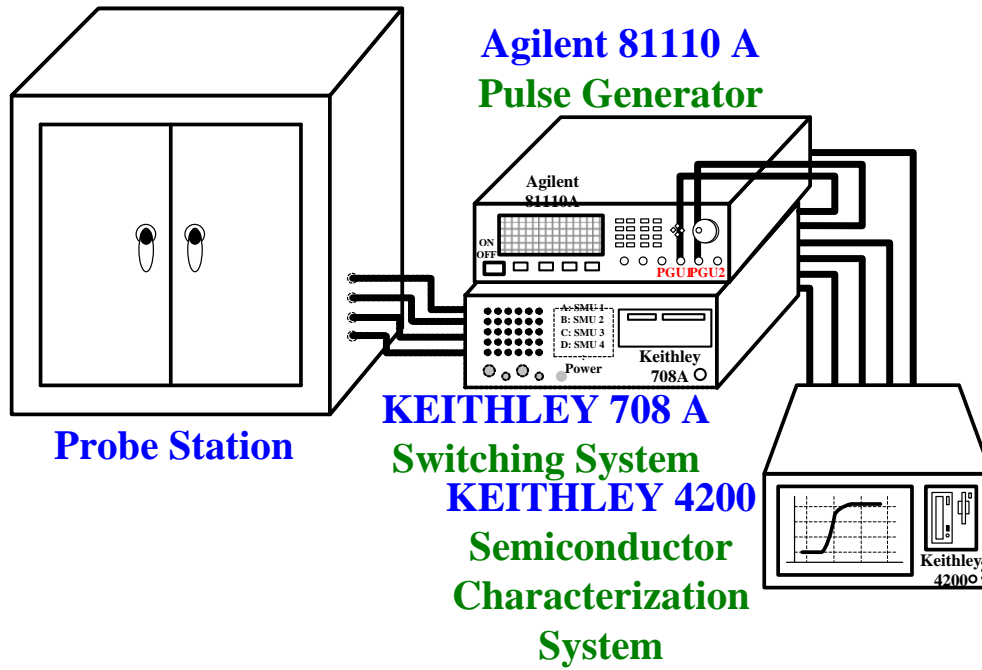
Fig. 2-9   The experimental setup of each apparatus for I-V characteristics

measurement.

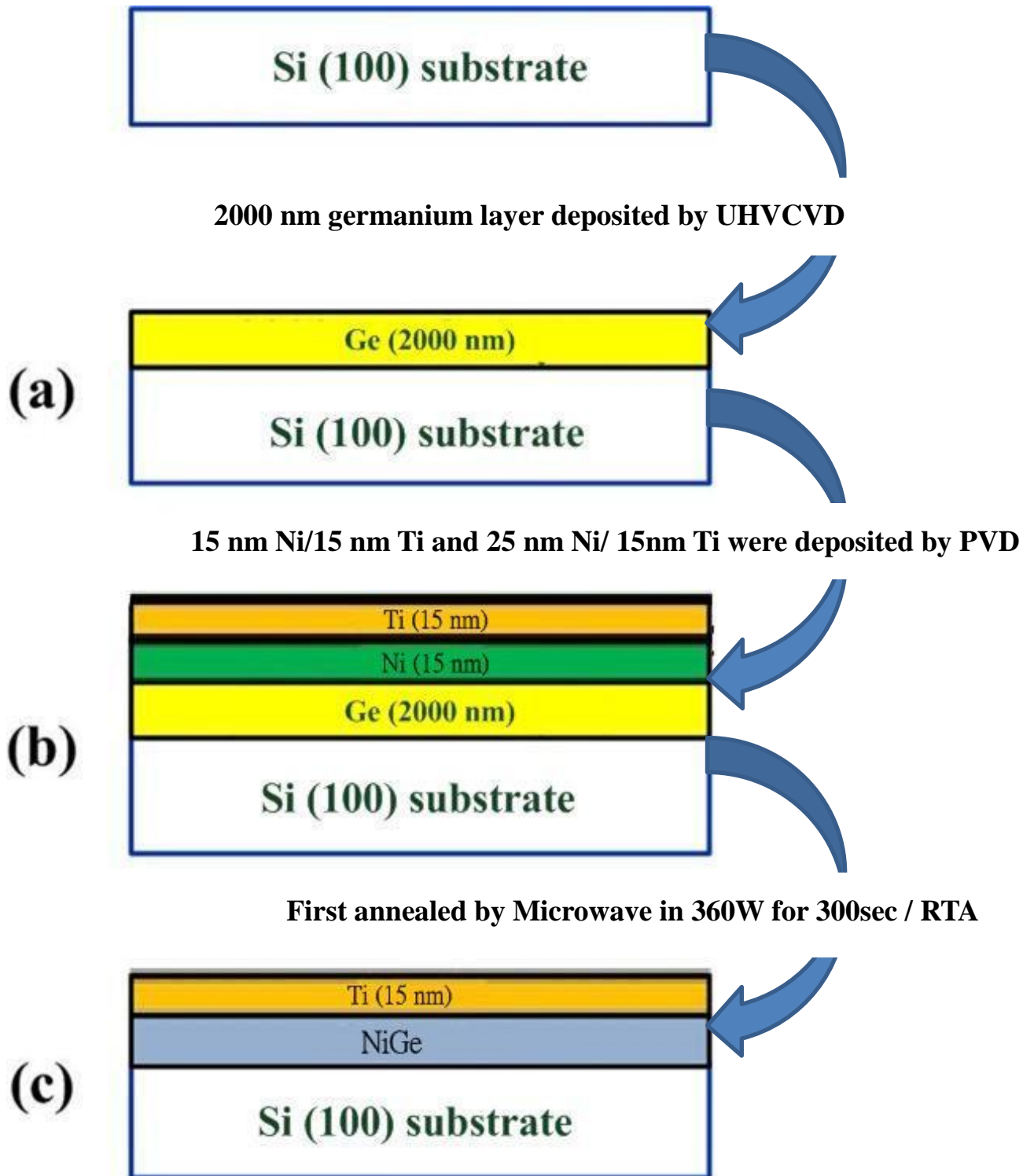| Microwave calculations				
	Conductivity $(\frac{S}{m})$	Permeability $(\frac{H}{m})$	Attenuation constant $(\frac{Np}{m})$ $\alpha = \sqrt{\pi\mu f\sigma}$	Traveling decay $\delta = E_0(1 - e^{-\alpha z})$
Ni (15nm)	$\sigma_{Ni} = 14.3 \times 10^6$	$\mu_{Ni} = 125 \times 10^{-6}$	$\alpha_{Ni} = 5.7 \times 10^6$	$\delta_{Ni} = 0.09E_0 =$ 9% loss (= 91% remaining)
Ti (15nm)	$\sigma_{Ti} = 2.38 \times 10^6$	$\mu_{Ti} = \mu_0 = 4\pi \times 10^{-7}$	$\alpha_{Ti} = 2.3 \times 10^7$	$\delta_{Ti} = 0.003E_0 = 0.3\%$ loss (= 99.7% remaining)
Si (695μm)	$\sigma_{Si} = 5$	$\mu_{Si} = \mu_0 = 4\pi \times 10^{-7}$	$\alpha_{Si} = 338.3$	$\delta_{Si} = 0.21E_0 = 21\%$ loss (= 79% remaining)

Table 2- 1 Numerical data of the materials is contained to calculate attenuation

constant and traveling decay. Power decay is much apparent in Ni layer.

Chapter 3

Results and Discussion

3.1 Introduction

As the urgent demand of thickness − resistance for Ni silicide as ITRS requirements, we are here in this chapter to provide the solution. The results of blanket Ni silicide formed by MWA/RTA, 90 nm pMOSFET device and blanket Ni germanide formed by MWA will be presented and elaborated. For the results of blanket Ni silicide, the primary concern is the relation between sheet resistance, thickness, and temperature with respect to different annealing conditions. Downscaled silicide thickness, lower sheet resistance and much more stable phase are what we are after. For 90 nm pMOSFET device, the improvement on I-V curve and leakage will be presented and detailed as well. Moreover, Ni germanide, as regarded as the materials for next generation, is formed by microwave annealing for the first time.

3.2 The ultrathin blanket Ni silicide formed by only MWA

A series of splits using MWA only is performed and summarized in Table 3-1. Splits vary in power levels, one or two step MWA, and setup 1 versus setup 2. M1 is the Ni silicide formed by only one-step 360W MWA in setup 1 for 300sec. M2 and M3 are formed by two step MWA. The first step of M2 and M3 are as the same as M1, but different in the second step annealing conditions. The second step annwaling of M2 and M3 are 600W in setup 2 for 300sec and 1300W in setup 2 for 300sec, respectively.　M4 is the Ni silicide formed by only one-step 360W MWA in setup 2

for 300sec. M4 and M5 are formed by two step MWA. The first step of MM5 and M6 are as the as M4, but different in the second step annealig conditions. The second step annealing of M5 and M6 are 600W in setup 2 for 300sec and 1300W in setup 2 for 300sec, respectively. The plot of the sheet resistance versus temperature for each condition is shown in Fig. 3-1. Sheet resistance compared to M4 (180 ohm/sq.), M1 (450 ohm/sq.) is much higher due to the relatively lower temperature in setup 1 than in setup 2. For M2 and M3 with the same first annealing condition to M1, stronger power (higher temperature) applied as second step annealing results in lower sheet resistance, which are 180 (ohm/sq.) and 100 (ohm/sq.) respectively. For M4 and M5 with the same first annelaing condition to M4, stronger power (higher temperature) applied as second step annealing results in lower sheet resistance, which are 100 (ohm/sq.) and 20 (ohm/sq.) respectively. So far, extremely low sheet resistance has achieved in condition M6.

The plot of the sheet resistance versus silicide thickness for each condition is shown in Fig. 3-2. Higher sheet resistance usually results in thin silicide thickness. Silicide thickness compared to M4 (9nm), M1 thus reached ultrathin silicide thickness (3.2nm) with its high sheet resistance. For M2 and M3 with the same first annealing condition to M1, the sheet resistance is dramatically declined with very little increment of thickness, which are 4.7 nm and 6.5 nm from 3.2nm respectively. For M4 and M5 with the same first annealing condition to M4, the same conccept is confirmed as well. The sheet resistance is dramatically declined with very little increment of thickness, which are 10 nm and 10.5nm from 9 nm respectively.

Now we concentrate the concern into phase issue. The conventional tool for phase examinaiton is by XRD, however, the thickness formed by MWA is too thin to detect. Therefore, selective area diffraction pattern (SADP) is applied to confirm the

phase of ni silicde. SADP is a crystallographic experimental skill that could be performed inside the transmission electron microscope (**TEM**), the image on the screen of the TEM will be a series of spots each spot corresponding to a satisfied diffraction condition of the sample's crystal structure. As shown in Table 3-2, smaller spots surrounded with red halo-shaped stand for the diffraction pattern of NiSi. The large and bright spots stand for the diffraction pattern of Si. The result of SADP indicates that amorphous phase of Ni silicide in M1 due to no ring pattern was discovered. For M2 and M4-M6, the phase of Ni silicide is indicated to be NiSi die to the existence of the ring pattern, and they could be further confirmed by EDS analysis as shown in Fig. 3-3. However, specific condition will result in the formation of $NiSi_2$, and its diffraction pattern right next to Si spot is specified in M3, the phase could also be confirmed by EDS as shown in Fig. 3-3. Fig. 3-4 will help to elaborate this phenomenon. The amorphous NiSi phase of M1 is transformed to $NiSi_2$ after second step MWA with formation of $NiSi_2$ pyramids. M4 is in NiSi phase after the first step MWA in setup 2 at higher temperature than M1 (as Fig. 2-3 indicated), and M6 is also in NiSi phase after 2nd MWA with low sheet resistance. The second step MWA drives Ni to redistribute in the silicide instead of penetrating into the underlying Si because the NiSi phase is formed in the first step. The thermal budget of the second step MWA is sufficient to transform the original silicide into NiSi films without increasing the silicide thickness.

3.3 The blanket Ni silicide film formed by RTA and MWA

In this section, a series of splits comparing first step RTA and second step (RTA/MWA) annealing are summarized in Table 3-3. C1 is the Ni silicide formed by only one-step RTA in $180^{o}C$ for 15sec. The first step of C2 and C3 are as the same as

C1, but different in the second step annealing conditions. The second step annwaling of C2 and C3 are in RTA 600$^{\rm o}$C for 15sec and MWA 2000W in setup 2 for 300sec, respectively. C4 is the Ni silicide formed by only one-step RTA in 260$^{\rm o}$C for 15sec. The first step of C5 and C6 are as the same as C4, but different in the second step annealing conditions. The second step annwaling of C5 and C6 are in RTA 450$^{\rm o}$C for 15sec and MWA 1300W in setup 2 for 300sec, respectively. The plot of the sheet resistance versus temperature for each condition is shown in Fig. 3-5. Sheet resistance compared to C4 (78 ohm/sq.), C1 (400 ohm/sq.) is much higher due to the lower temperature in first-step of RTA. For sheet resistance in C2 (83 ohm/sq.) is alomost identical to C3 (79.3 ohm/sq.), which suggests the same sheet resistance for 600$^{\rm o}$C RTA to achieve simply requires 420$^{\rm o}$C for MWA. For sheet resistance in C5 (8 ohm/sq.) is a little higher than C6 (6.37 ohm/sq.) even annealing temperature for C6 is lower than C5, which reveals that ultalow sheet resistance for MWA to achieve merely requies 360$^{\rm o}$C. These results indicates that MWA meet the current requirements and tendency of low-temperatur e in downscaled device fabrication.

The plot of the sheet resistance versus silicide thickness for each condition is shown in Fig. 3-6. Higher sheet resistance usually results in thin silicide thickness, consistent as the data in seciton 3.2. Silicide thickness compared to C4 (18.09nm), C1 thus reached extremely thin silicide thickness (5.42nm) due to its lower first annealing temperature in RTA. Besides lower second step annealing temperature, C3(6.84 nm) is even thinner than C2 (7.03 nm) for their silicide thickness. For C5 and C6 with the same first annealing condition to C4, silicide thickness for C6 is thinner than C5 with their sheet resistance both declined from 78 (ohm/sq) to less than 10 (ohm/sq.). However as shown in Table 3-4, specific anneal condiiton such as C2 and C3 will result in the formation NiSi$_2$ which will lead to great leakage in ultra shallow

junction (USJ).

Therefore here we concentrate the concern into phase issue, again. For silicide thickness is less than 10nm in the case of C1-C3, SADP and EDS are applied to analysis the phase as shown in Table 3-5. The composition for Ni:Si is almost 2:1 for C2 and C3 which indicates that the phase of Ni silicide is $NiSi_2$, and is consistent to the SADP pattern. For silicide thickness is not less than 10 nm, XRD is able to examine the phase for each condition. As shown in Fig. 3-7, the phase of C4, C5 and C6 are Ni_2Si, NiSi and NiSi including corresponded orientation. Besides, the phase of M6 is also able to be detected by XRD due to its complete transformation into NiSi as shown in Fig. 3-7.

3.4 The reliability examination

A post thermal process is demonstrated in order to examine the thermal reliability of the silicide formed by microwave annealing. As identified in Fig. 3-8, other than   good thermal stability of M6 (10.5 nm NiSi) is expected to at least 600 ℃.

3.5 90 nm pMOSFET Device

So far, the results from the blanket silicide formed by microwave annealing are optimistic and promising. Therefore, we applied two-step MWA into the fabrication process of 90 nm pMOSFET devices. Its results are presented and elaborated in this section.

Fig. 3-9 identifies the sheet resistance of poly-gate lines for splits of C4, M4 and M6 as a function of gate width. As the gate lines are reduced to 30 nm, sheet resistance is still low for the two-step MWA process, which implies its compatibility

in the downscaled fabrication process. Fig. 3-10 shows that silicide of M6 with two step MWA, relative to a no silicide control, improves the MOSFET on and off current and the diode junction leakage. Fig. 3-11 shows that the drain current is increased by 110% for the M6 silicide applied.

3.6 The blanket Ni germanide film formation

In this section, we primarily discuss the formation of Ni germanide by MWA and RTA respectively.

3.6.1 The blanket Ni germanide film formed by MWA

As shown in Table 3-6, thickness of NiGe can be measured from TEM with different thickness of Ni layer deposited on germanium epitaxial layer. Before MWA takes place, Ni/Ti =15/15nm is deposited for G1 and Ni/Ti =25/15nm is deposited for G2. From the top of the TEM, there are films of TiN (15nm), NiGe, Ge layer and Si substrate respectively. The thickness of Ni germanide for G1 and G2 are 57 nm and 72nm. We can observe that both of the Ni is fully reacted with Ge during microwave annealing, so thicker Ni layer deposited results thicker Ni germanide thickness.

3.6.2 The blanket Ni germanide film formed by RTA

As shown in Table 3-7 , thickness of NiGe can be measured from TEM with different thickness of Ni layer deposited on germanium epitaxial layer. After Ni/Ti = 15/15nm deposited on Ge layer, various annealing temperature from 350°C to 650°C of RTA for 30sec take place to form NiGe. From the top of the TEM, there are films of Ti (15nm), NiGe, Ge layer and Si substrate respectively. The thickness of G3 (RTA 350°C), G4 (RTA 450°C), G5 (RTA 550°C) and G6 (650°C) are 38.63 nm, 48 nm,

50.83 nm and 125 nm, respectively. We can observe the same phenomenon, which is that all of the Ni is fully reacted with Ge during RTA; therefore, thicker Ni layer deposited results in thicker Ni germanide thickness, just the same as the trend of microwave annealing suggests. Moreover, the phase of NiGe is verified in Fig. 3-12, we can observe that only NiGe phase formed in the range of 350°C to 650°C. As identified in Fig. 3-13 ~ Fig. 3-16, the results of Secondary Ion Mass Spectroscopy (SIMS) is presented in order to further examine the detail distribution of Ni, Ti and Ge. It is reasonable that wilder Ni profile is due to the more thermal budget, which also leads to thicker Ni germanide thickness.
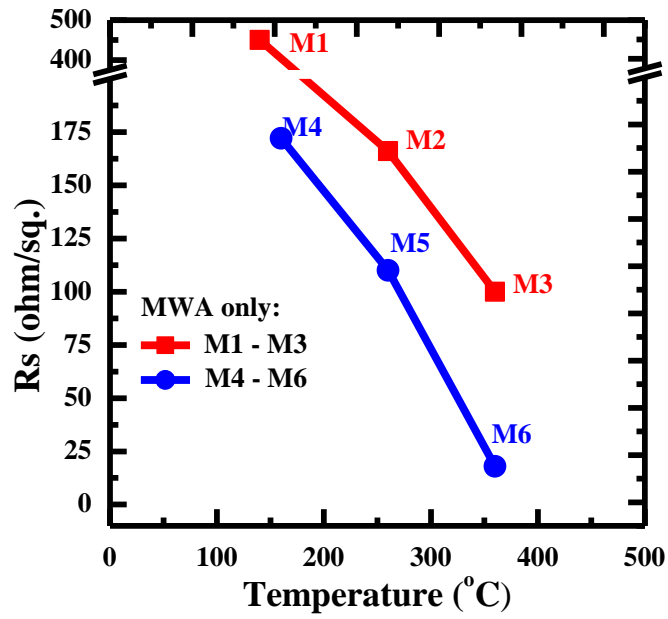
Fig. 3- 1   The plot of Rs to Temperature for the split M1 to M6, which indicates the

Rs drop as annealing temperature increased.
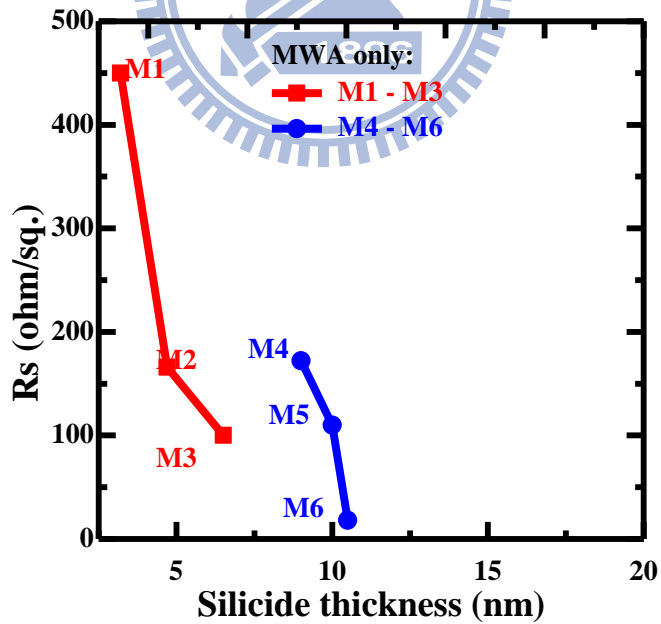
Fig. 3- 2   The plot of Rs to thickness for the split M1 to M6, and M6 appeared to

have lower sheet resistance and ultrathin silicide thickness.
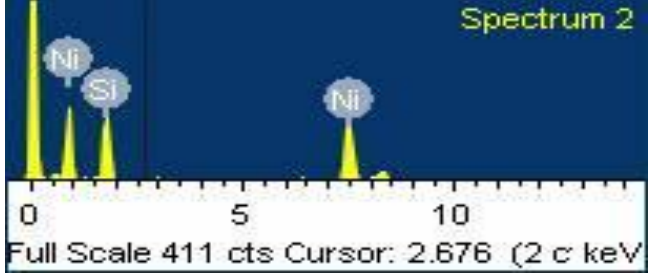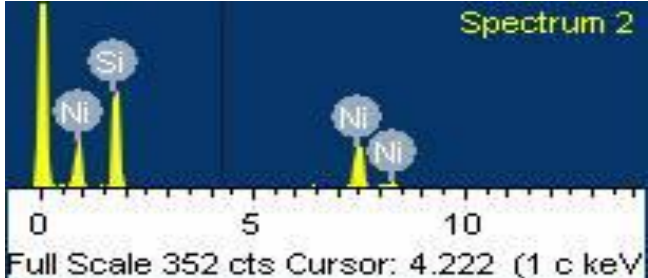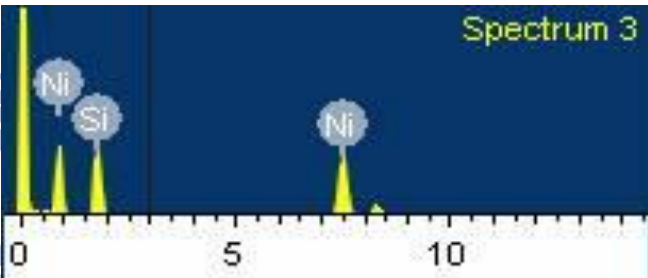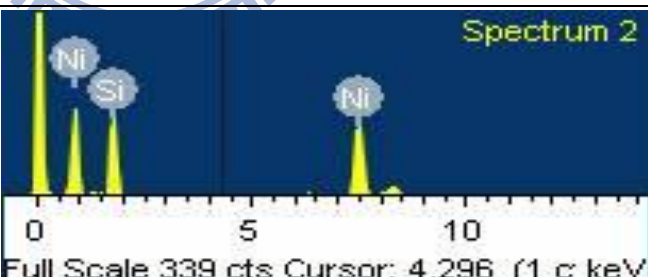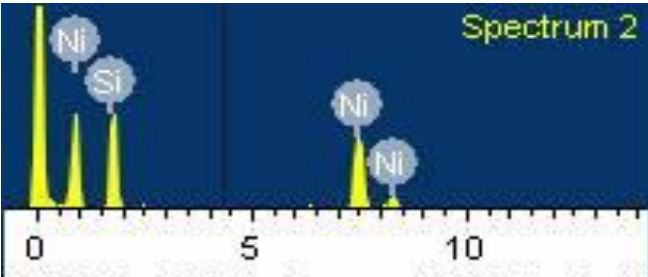
Set			Spectrum
M2			
Element	Si at. %	Ni at. %	
Compose	52.92	47.08	
M3			
Element	Si at. %	Ni at. %	
Compose	69.22	30.78	
M4			
Element	Si at. %	Ni at. %	
Compose	51.81	48.19	
M5			
Element	Si at. %	Ni at. %	
Compose	51.54	48.46	
M6			
Element	Si at. %	Ni at. %	
Compose	55.46	44.54	

Fig. 3- 3   The table contains the analysis of EDS to confirm the composition of splits.

32
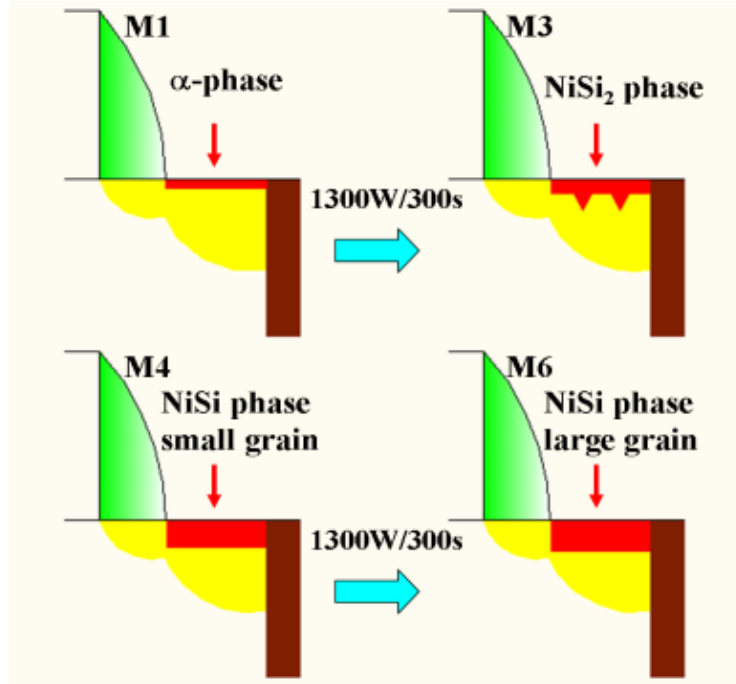
Fig. 3- 4   Second step MWA results in redistributing in the silicide instead of

penetrating into the underlying Si if the NiSi phase is formed in the first step.
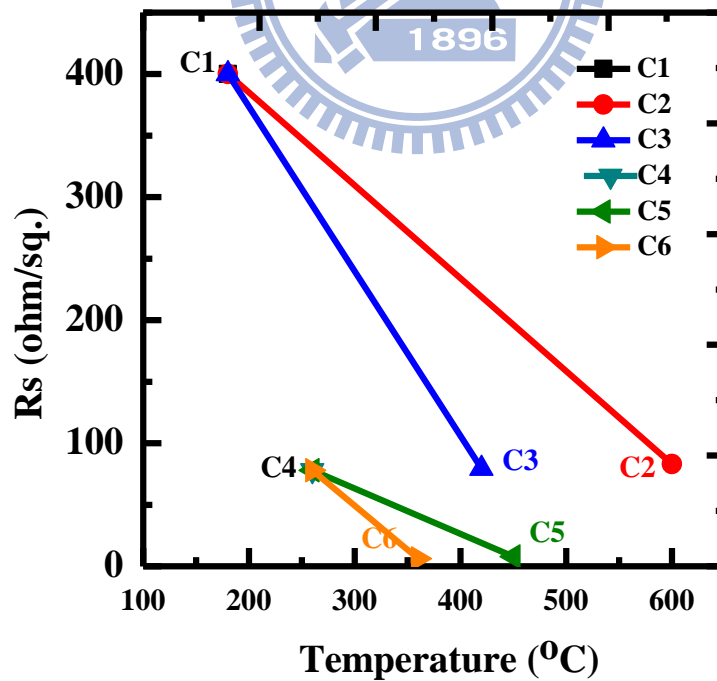
Fig. 3- 5   The plot of Rs to Temperature for the split C1 to C6. The same with

M-series, higher annealing temperature will lead to lower sheet resistance.
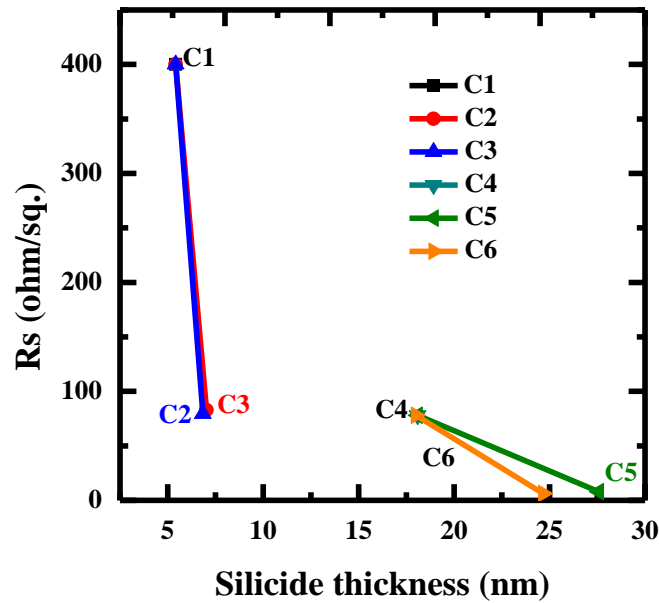
Fig. 3- 6 The plot of Rs to thickness for the split C1 to C6. C2 and C3 appeared to have the same thickness and Rs, but lower temperature required in C2. C5 and C6 appeared to have low Rs, but their silicide thickness is too thick.
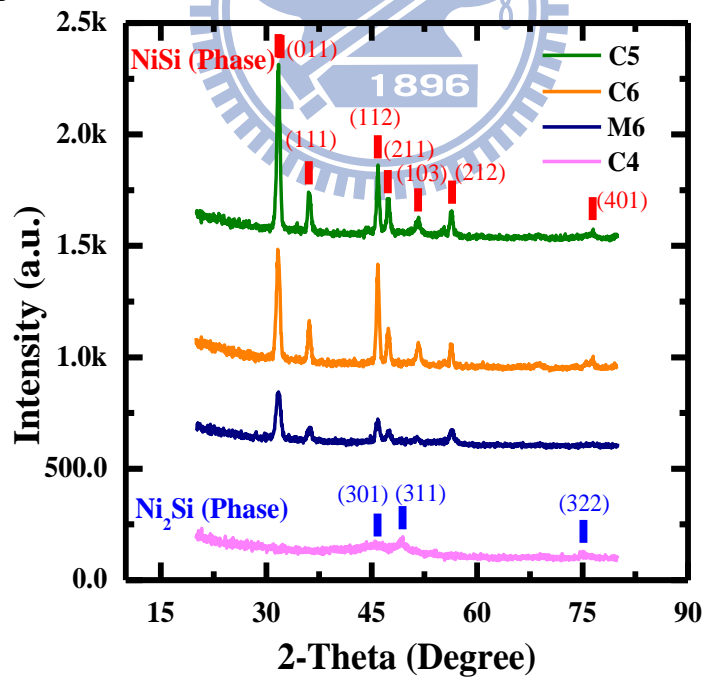
Fig. 3- 7 The GIXRD figure to confirm the phase of C4, C5, C6 and M6
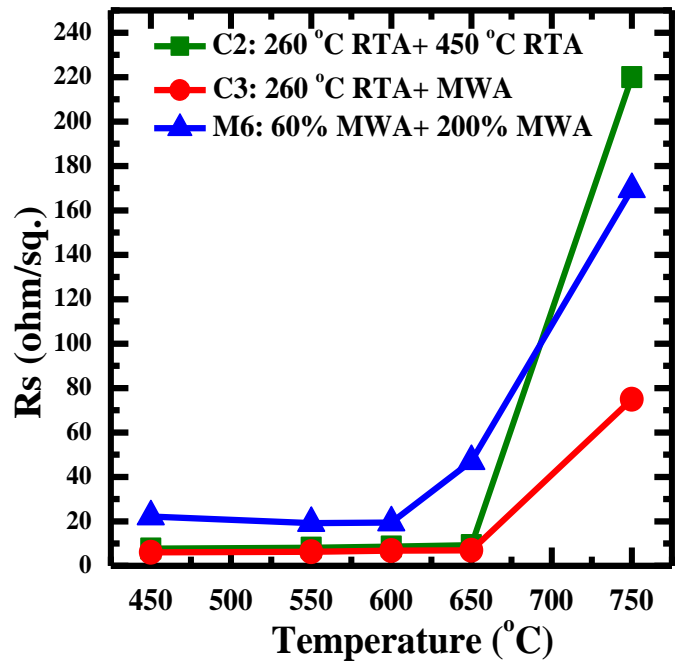
Fig. 3- 8   The plot of thermal stability for various temperature. It shows M6 still
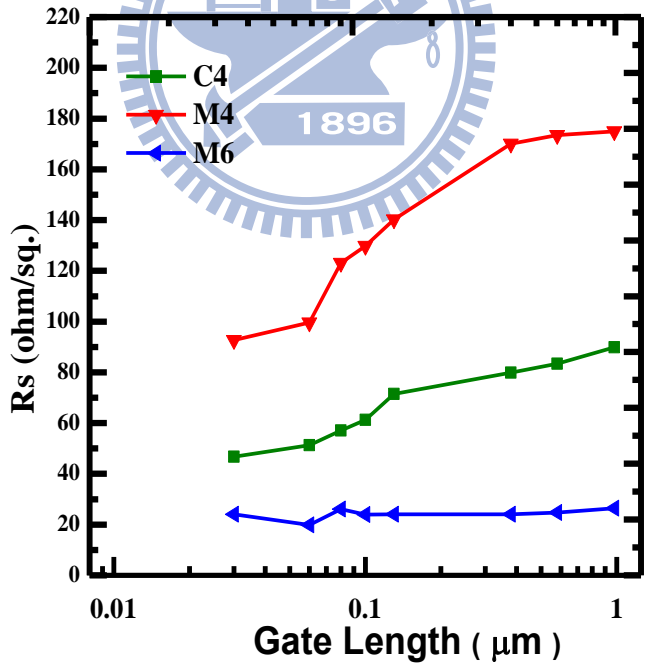
remains good thermal stability until $600^{o}C$

Fig. 3- 9   Rs at poly-gate lines for C4, M4 and M6 silicide as a function of width,

which indicates the silicide formed in condition M6 remains low Rs as the downscale
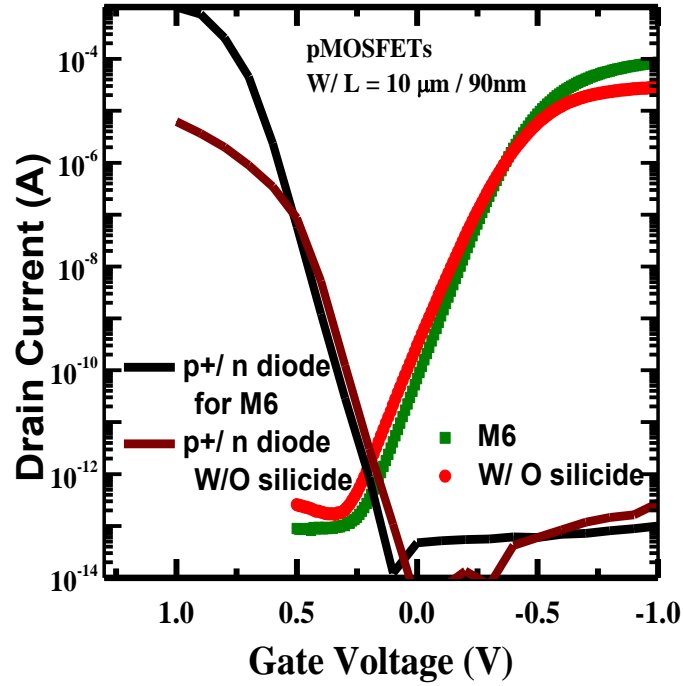
of gate length

Fig. 3- 10 I_D-V_G of pMOSFETs and I- V of p+/n diode for M6 and W/O silicide. M6

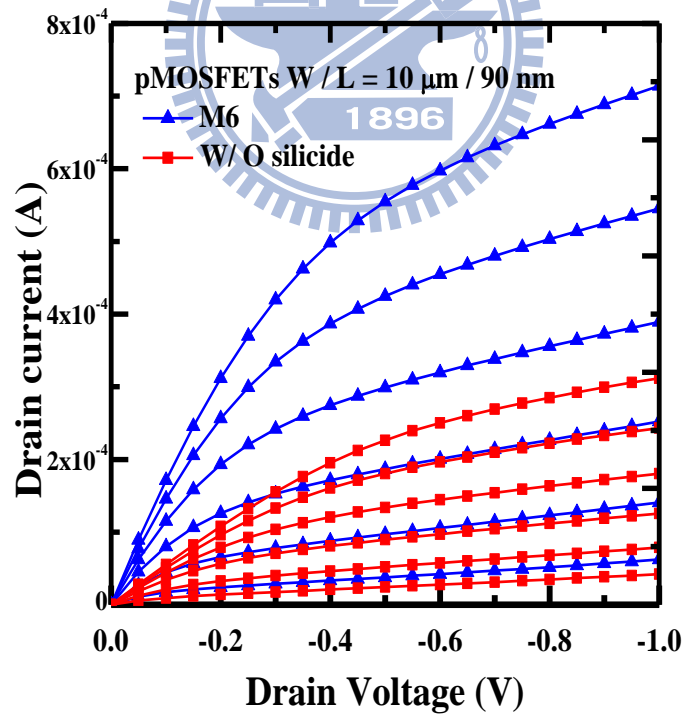improves the MOSFET on and off current and the diode junction leakage.

Fig. 3- 11 I_D-V_D of pMOSFETs for M6 and W/O silicide. Drain current increased by
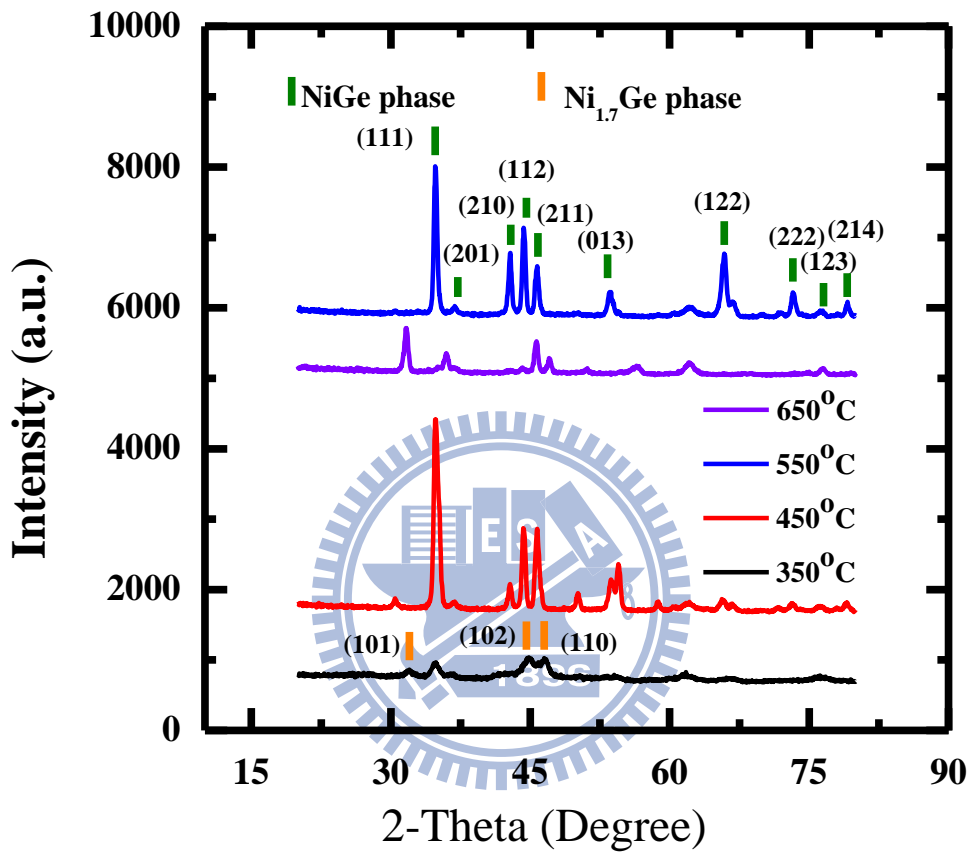
110% by M6 silicide.

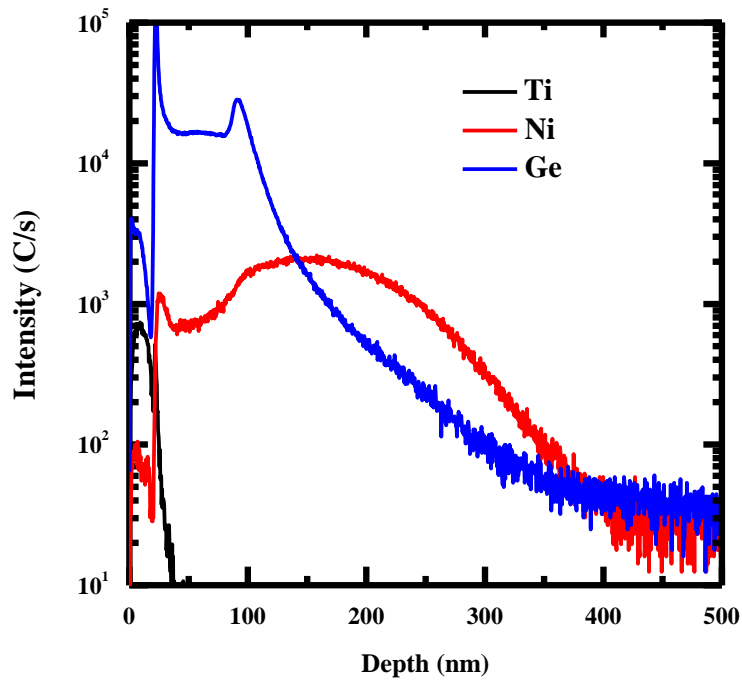Fig. 3- 12 The GIXRD figure to verify the phase of Ni germanide

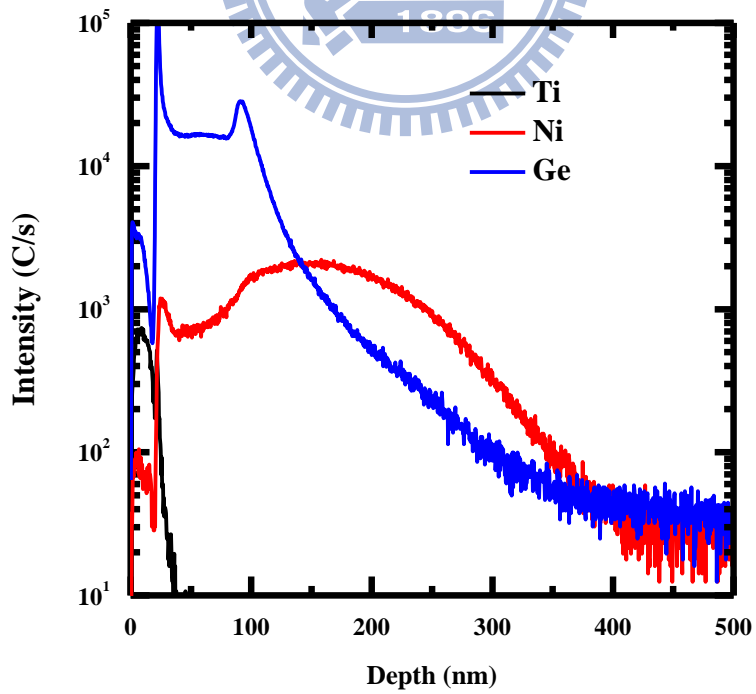Fig. 3- 13   The SIMS of NiGe in RTA 350°C

Fig. 3- 14   The SIMS of NiGe in RTA 450°C
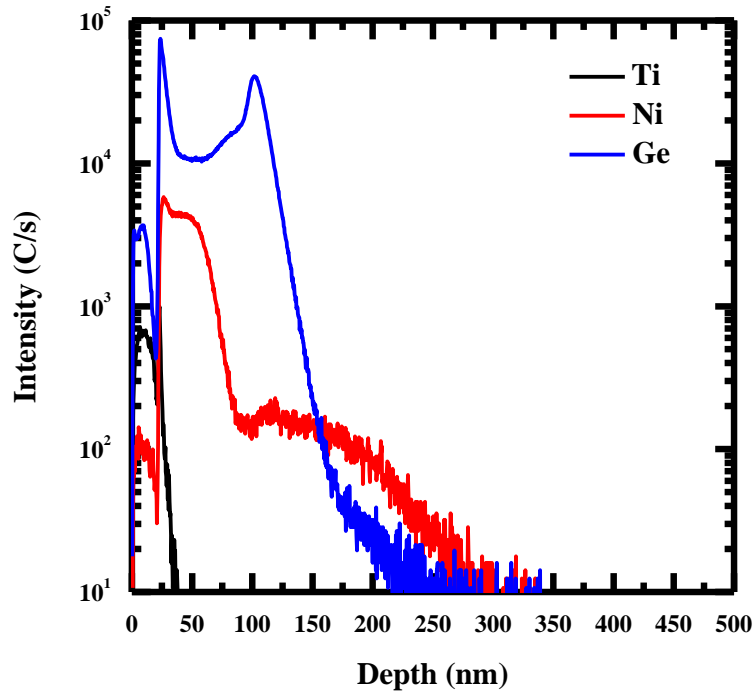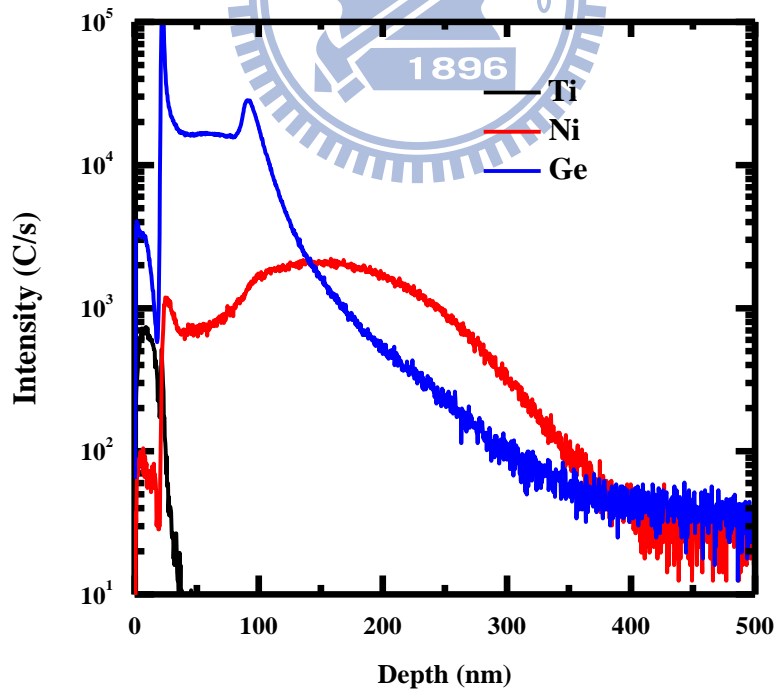
Fig. 3- 15   The SIMS of NiGe in RTA 550°C

Fig. 3- 16   The SIMS of NiGe in RTA 650°C

	Steps of MWA	First step	Second step
		Power/Duration in Setup#	Power/Duration in Setup#
M1	1	60%/5mins in Setup 1	
M2	2	60%/5mins in Setup 1	100%/5mins in Setup 2
M3	2	60%/5mins in Setup 1	200%/5mins in Setup 2
M4	1	60%/5mins in Setup 2	
M5	2	60%/5mins in Setup 2	100%/5mins in Setup 2
M6	2	60%/5mins in Setup 2	200%/5mins in Setup 2

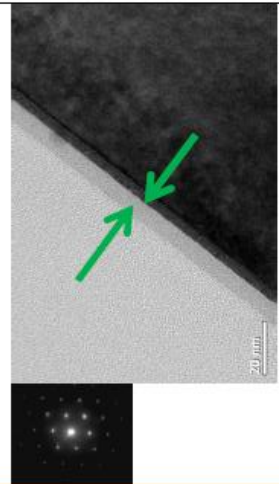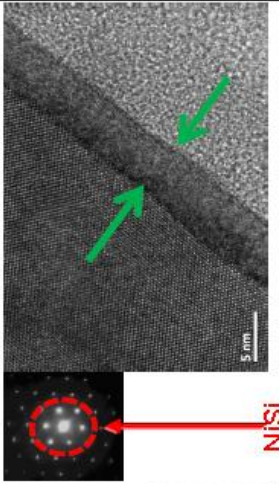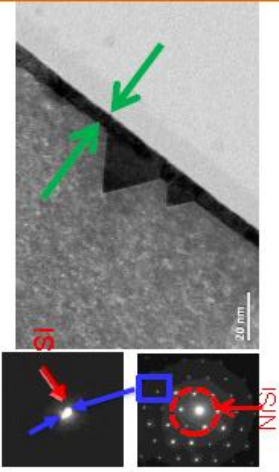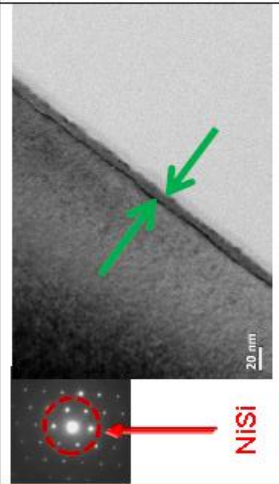Table 3- 1   The split table of M1 ~ M6
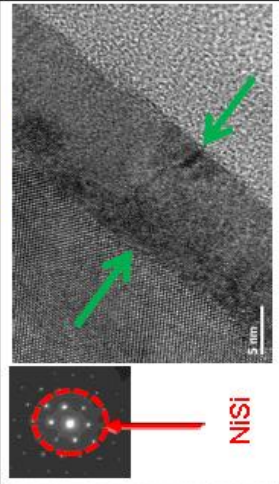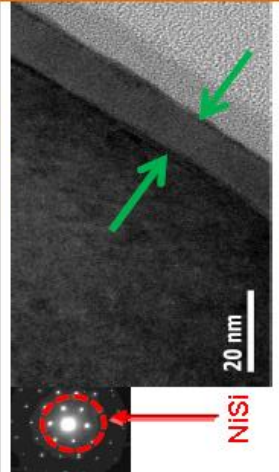
Set #	M1	M2	M3
First step	60%/5mins in Setup 1	60%/5mins in Setup 1	60%/5mins in Setup 1
Second step		100%/5mins in Setup 2	200%/5mins in Setup 2
Diffraction Pattern			
$T_{silicide}$	3.2nm	4.7nm	6.5nm
Summary	No any NiSi spot discovered	NiSi pattern discovered	NiSi and NiSi$_2$ pattern discovered

Set#	M4	M5	M6
1st step	60%/5mins in Setup 2	60%/5mins in Setup 2	60%/5mins in Setup 2
2nd step		100%/5mins in Setup 2	200%/5mins in Setup2
Diffraction pattern			
$T_{silicide}$	9nm	10nm	10.5nm
Summary	NiSi pattern discovered	NiSi discovered	NiSi discovered

Table 3- 2   Ultra-thin NiSi silicide formed by both one-step and two-step MWA, M6 appeared to have the thinnest silicide.

	Steps of MWA	First step	Second step
		RTA/Duration	RTA / MWA
C1	1	180°C/15sec	
C2	2	180°C/15sec	RTA 600°C/15sec
C3	2	180°C/15sec	2000W/5mins in Setup 2
C4	1	260°C/15sec	
C5	2	260°C/15sec	RTA 450°C/15sec
C6	2	260°C/15sec	1300W/5mins in Setup 2

Table 3- 3   The splits table of C1 ~ C6
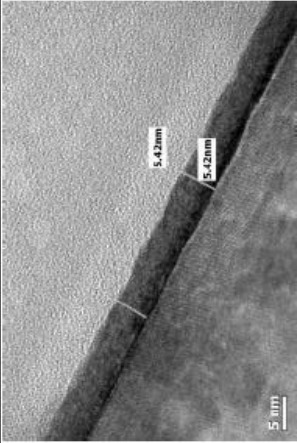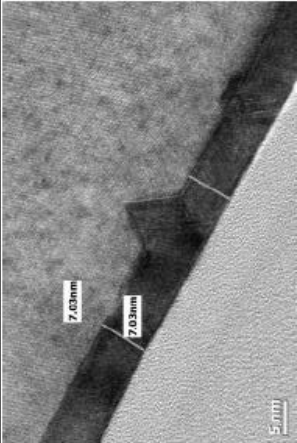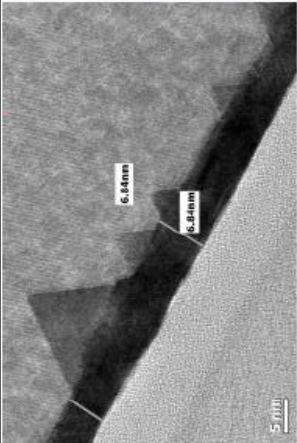
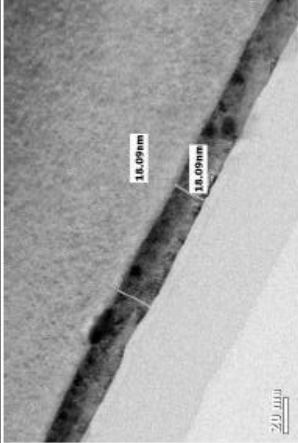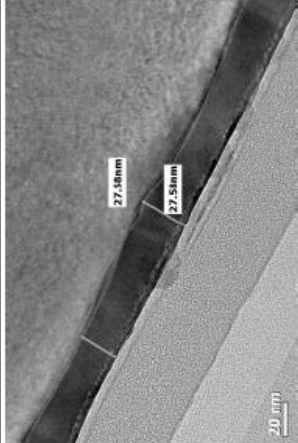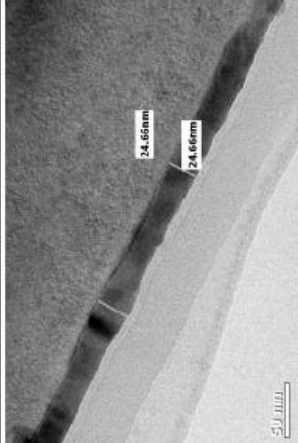|	C1	C2	C3
Set #			
First step	RTA 180°C/15sec	RTA 180°C/15sec	RTA 180°C/15sec
Second step		RTA 600°C/15sec	2000W/5mins in Setup 2
TEM	(5.42nm)	(7.03nm)	(6.84nm)
$T_{silicide}$	5.42 nm	7.03 nm	6.84 nm
Summary	Ni₂Si	NiSi₂	NiSi₂

	C4	C5	C6
Set#			
First step	RTA 260°C/15sec	RTA 260°C/15sec	RTA 260°C/15sec
Second step		RTA 450°C/15sec	1300W/5mins in Setup 2
TEM	(18.09nm)	(27.58nm)	(24.66nm)
$T_{silicide}$	18.09 nm	27.58 bn	24.66 nm
Summary	Ni₂Si	NiSi	NiSi

Table 3- 4   The comparison table of silicide formed by MWA/RTA. Compared to microwave, silicide formed by RTA is suffered from unstable phase and thickness.
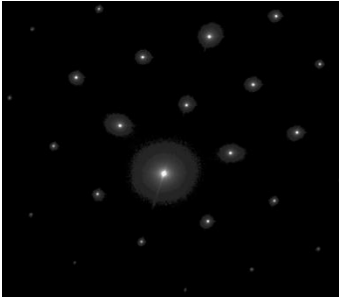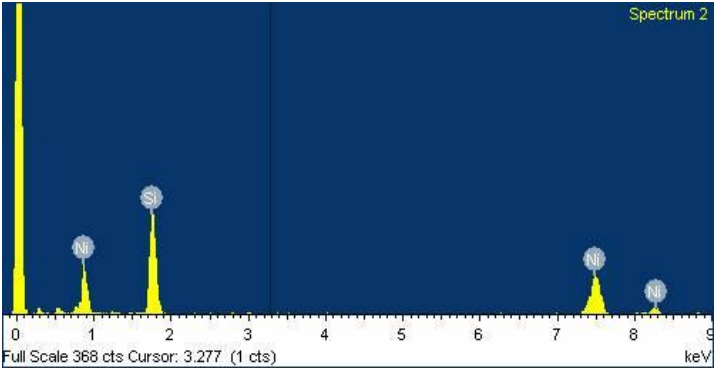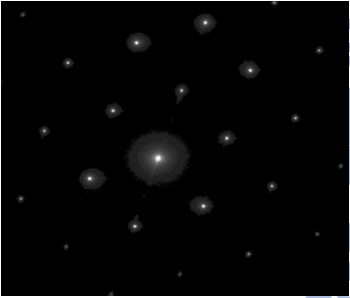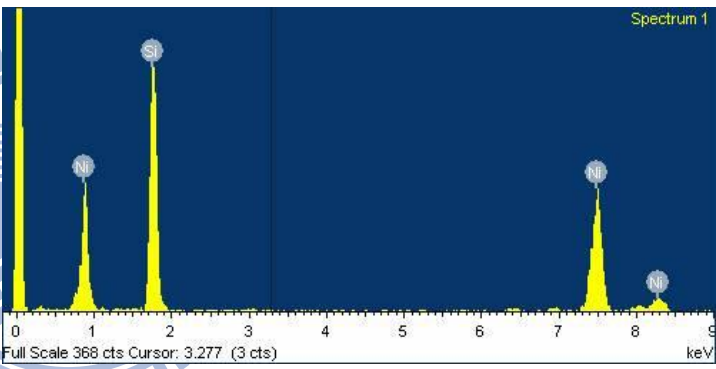
Set#	C2	
Analysis	**SADP**	**EDS**
Diffraction Pattern		Spectrum 2 Full Scale 368 cts Cursor: 3.277 (1 cts)
Comment	**Ni silicide is NiSi₂ by SADPs.**	**Composition** **69.37 at. % Si, 30.63 at.% Ni**
Set#	C3	
Analysis	**SADP**	**EDS**
Diffraction Pattern		Spectrum 1 Full Scale 368 cts Cursor: 3.277 (3 cts)
Comment	**the Ni silicide is NiSi₂ by SADPs.**	**Composition** **67.15 at. % Si, 32.85 at.% Ni**

Table 3- 5   The table contains EDS and SADP data to confirm the phase

44
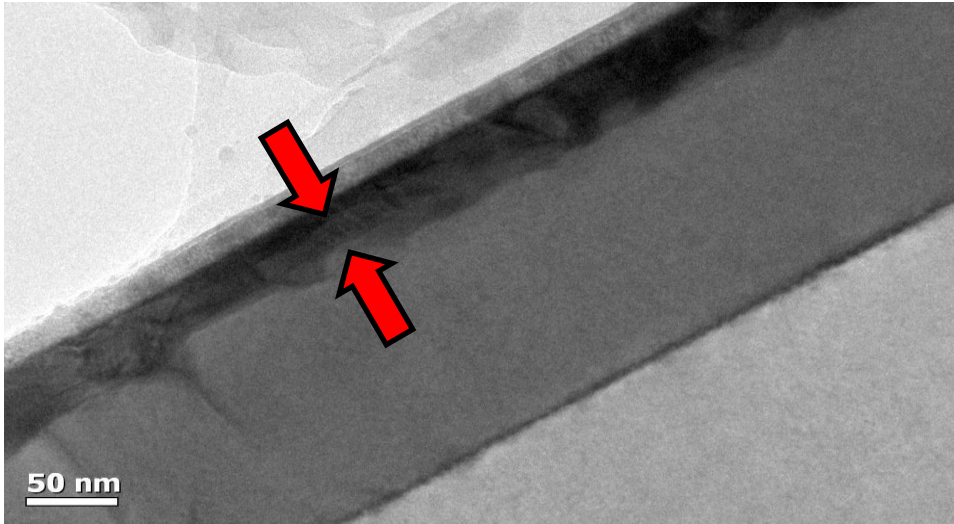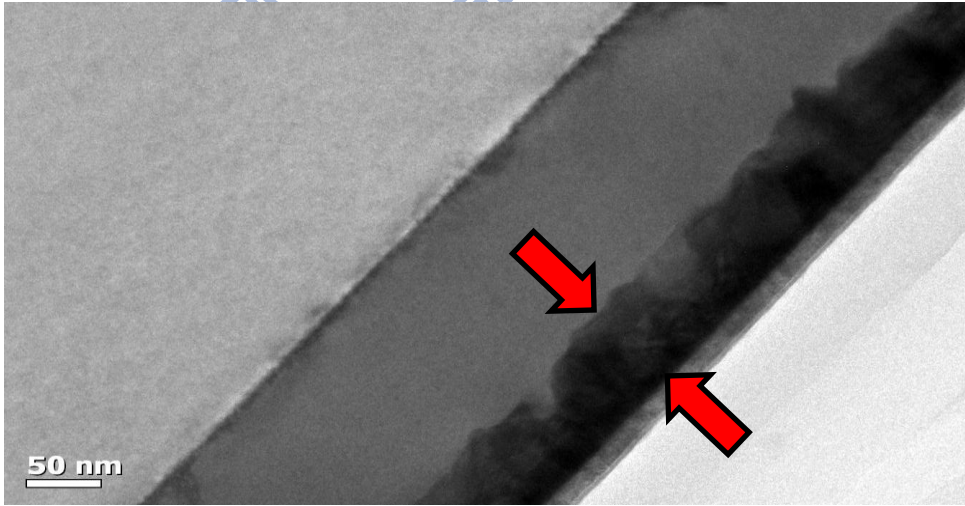
Set #	G1
Ni/Ti (nm)	15/15
Annealing	360W MWA in setup 1 for 5mins
TEM	
T germanide	57 nm
Phase	NiGe
Set#	G2
Ni/Ti (nm)	25/15
Annealing	360W MWA in setup 1 for 5mins
TEM	
T germanide	72nm
Phase	NiGe

Table 3- 6 The table contains the TEM of NiGe formed by MWA
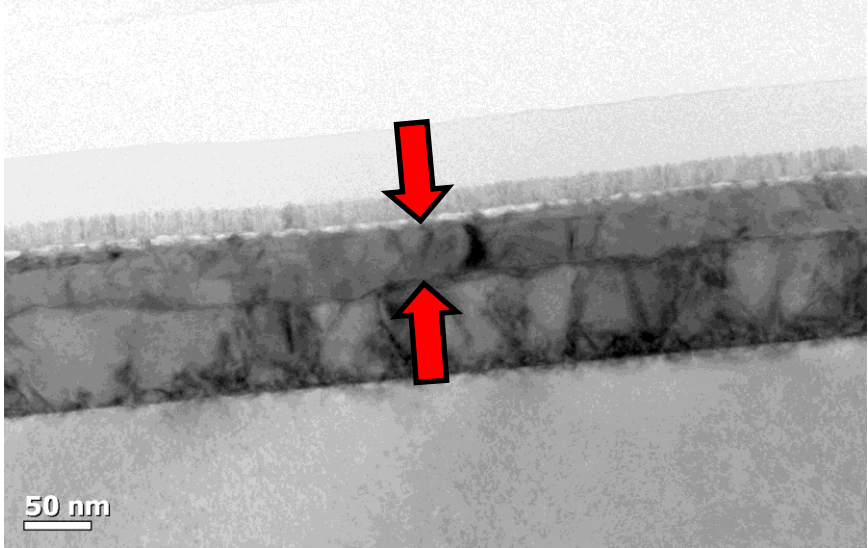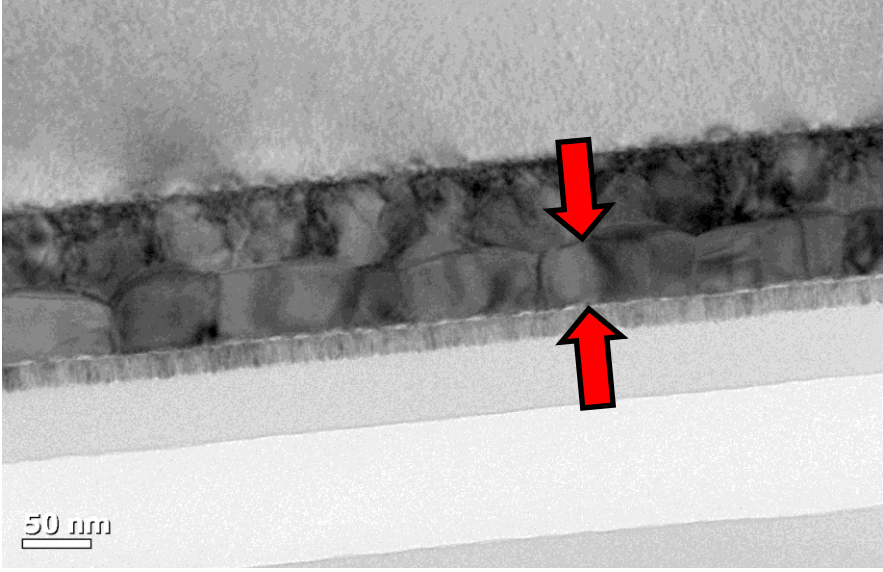
Set #	G3
Ni/Ti (nm)	15/15
Annealing	350°C RTA for 30sec
TEM	
T germanide	38.63 nm
Phase	NiGe, Ni$_{1.7}$Ge
Set#	G4
Ni/Ti (nm)	15/15
Annealing	450°C RTA for 30sec
TEM	
T germanide	48 nm
Phase	NiGe

Table 3- 7   The table contains the TEM of NiGe formed by RTA in 350°C and 450°C
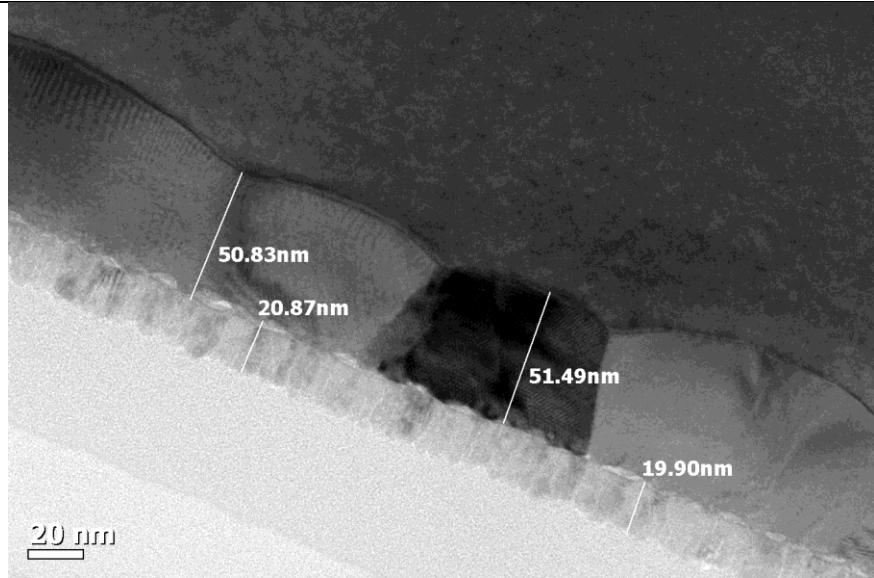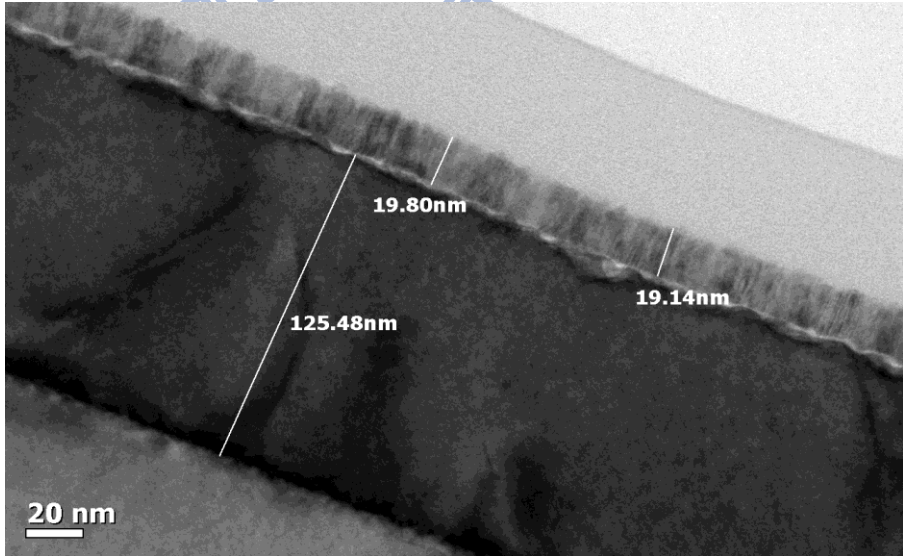
Set #	G5
Ni/Ti (nm)	15/15
Annealing	550°C RTA for 30sec
TEM	
T germanide	50.83 nm
Phase	NiGe
Set#	G6
Ni/Ti (nm)	15/15
Annealing	650°C RTA for 30sec
TEM	
T germanide	125.5 nm
Phase	NiGe, Ni$_3$Ge$_2$, Ni$_3$Ge

Table 3- 8   The table contains the TEM of NiGe formed by RTA in 550°C and 650°C

Chapter 4

Conclusions and Future Work

4.1 Conclusions

This thesis reports a novel silicide process that achieves Ni silicide thickness of 10.5 nm while maintaining low resistance of 18 ohm/sq. with 2-step low temperature MWA. This approach creates a very thin crystaline NiSi silicide film with the first MWA and a low resistance large grain NiSi phase without Ni penetration into Si with the second MWA. The Ni silicide formed by two-step MWA also exhibits to have thermal stability at least to 600°C. The ultra-thin Ni-silicide technology is thus able to meet the specifications of 2012-2021 single and multi-gate MPU/ASIC required by ITRS. Besides, this novel technique is also integrated into 90 nm pMOSFET device fabrication, and its improvement on I-V curve and leakage are both reported in this thesis as well. Moreover, NiGe formed by both MWA/RTA are presented and discussed in detail.

4.2 Future work

For recent years, microwave annealing technique integrated into device process procedure has offered a new solution for downscaled CMOS fabrication. That is the reason that more and more scientists and engineers are devoted in this area searching for improvements. In silicide formation issue, Ni silicide is still believed to be on its half way to thinner thickness, lower sheet resistance and more thermal stable phase. The solution is probably considered to be "three-step" microwave annealing. The

48

occasion applied three-step microwave annealing requires more discreet adjustments of power levels, setups in order to prevent the $NiSi_2$, which leads to great leakage in USJ. Furthermore, new material such as NiGe is regarded as a popular candidate for lowering sheet resistance in USJ for the future. Therefore, microwave annealing applied in dopant activation, silicide formation and low-temperature thermal process worth expecting for more.
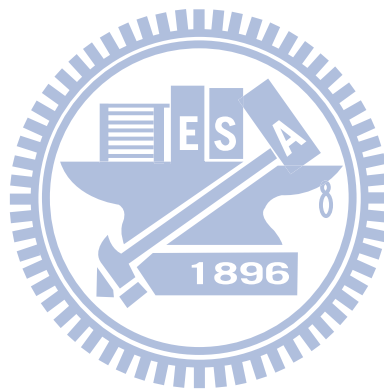
Reference

Chapter 1

[1.1] H. Iwai, T. Ohguro, and S. Ohmi., "NiSi salicide technology for scaled CMOS," Microelectronic Engineering, vol. 60, pp. 157-169, 2002.

[1.2] T. Morimoto, H. S. Momose, T. Iinuma, I. Kunishima, K. Suguro, H. Okano, I. Katakabe, H. Nakajima, M. Tsuchiaki, M. Ono, Y. Katsumata, and H. Iwai., "A NiSi salicide technology for advanced logic devices," in Electron Devices Meeting, 1991. IEDM '91. Technical Digest., International, 1991, pp. 653-656.

[1.3] K. Maex, G. Ghosh, L. Dalaey, V. Probst, P. Lippens, L. Van denhove, and R. F. De Keersmaecker., "Stability of As and B doped Si with respect to overlaying CoSi2 and TiSi2 thin films," Journal of Materials Research, vol. 4, pp. 1209-1217, 1989.

[1.4] V. Probst, H. Schaber, P. Lippens, L. Van den hove, and R. De Keersmaecker., "Limitations of TiSi2 as a source for dopant diffusion," Applied Physics Letters, vol. 52, pp. 1803-1805, 1988.

[1.5] B. Adams, D. Jennings, K. Ma, A. J. Mayur, S. Moffatt, S. G Nagy, and V. Parihar., "Characterization of Nickel Silicides Produced by Millisecond Anneals," in Advanced Thermal Processing of Semiconductors, 2007. RTP 2007. 15th International Conference on, 2007, pp. 155-160.

[1.6] M. Poon, F. Deng, M. Chan, W. Y. Chan, and S.S. Lau., "Resistivity and thermal stability of nickel mono-silicide," Applied Surface Science, vol. 157, pp. 29-34, 2000.

[1.7] K. Tsutsui, R. Xiang, K. Nagahiro, T. Shiozawa, P. Ahmet, Y. Okuno, M. Matsumoto, M. Kubota, K. Kakushima, and H. Iwai.., "Analysis of irregular increase

in sheet resistance of Ni silicides on transition from NiSi to NiSi2," Microelectronic Engineering, vol. 85, pp. 315-319, 2008.

[1.8] T. Iinuma, N. Itoh, K. Inou, H. Nakajima, S . Matsuda, I. Kunishima, K. Suguro, Y. Katsumata, and H. Iwai., "A self-aligned emitter base NiSi electrode technology for advanced high-speed bipolar LSIs," in Bipolar/BiCMOS Circuits and Technology Meeting, 1992., Proceedings of the 1992, 1992, pp. 92-95.

[1.9] G. Kim, D. Yoo, H. Baik, J. Myoung, S. Lee, S. Oh, and C. Park., "Improved thermal stability of Ni silicide on Si (100) through reactive deposition of Ni," Journal of Vacuum Science & Technology B: Microelectronics and Nanometer Structures, vol. 21, p. 319, 2003.

[1.10] K. De Keyser, C. Van Bockstael, R. L. Van Meirhaeghe, C. Detavernier, E. Verleysen, H. Bender, W. Vandervorst, J. Jordan-Sweet, and C. Lavoie., "Phase formation and thermal stability of ultrathin nickel-silicides on Si(100)," Applied Physics Letters, vol. 96, pp. 173503-3, 2010.

[1.11] R. Tung, J. M. Gibson, and J. M. Poate., "Formation of Ultrathin Single-Crystal Silicide Films on Si: Surface and Interfacial Stabilization of Si-NiSi2 Epitaxial Structures," Physical Review Letters, vol. 50, pp. 429-432, 1983.

[1.12] F. d'Heurle, C. S. Petersson, J. E. E. Baglin, S. J. La Placa, and C. Y. Wong., "Formation of thin films of NiSi: metastable structure, diffusion mechanisms in intermetallic compounds," Journal of Applied Physics, vol. 55, pp. 4208-4218, 1984.

[1.13] Kittl, J.A., Veloso, A., Lauwers, A.; et al. "Scalability of Ni FUSI gate processes: phase and Vt control to 30 nm gate lengths", VLSI Technology, 2005. Digest of Technical Papers. 2005 Symposium on p.72 - 73

[1.14] T. Yamaguchi et al., IEDM Tech. Dig., p.576-579, 2010

[1.15] C. Ortolland et al, IEDM Tech. Dig., p23-26, 2009

[1.16] B. Adams et al., RTP 2007. P.155, 2007

[1.17] J.P. Li et al, RTP 2009, p.1, 2009

[1.18] ITRS 2010

Chapter 2

[2.1] Yao-Jen Lee, Yu-Lun Lu, Fu-Kuo Hsueh, et al. "3D 65nm CMOS with 320℃ Microwave Dopant Activation", IEDM Tech. Dig., p31-34, 2009

[2.2] Yu-Lun Lu, Fu-Kuo Hsueh, Kuo-Ching Huang, Tz-Yen Cheng, et al. "Nanoscale p-MOS Thin-Film Transistor with TiN Gate Electrode Fabricated by Low-Temperature Microwave Dopant Activation", Electron Device Letters, IEEE, Volume: 31 Issue:5, p437 - 439 , 2010

[2.3] TaoWang, Yongbin Dai, Qingyuan Dai, et al. "Microwave plasma anneal to fabricate silicides and restrain the formation of unstable phases", Electron Devices and Solid-State Circuits, 2007, EDSSC 2007, p609 – 612.

[2.4] Alford, T. L.; Thompson, D. C.; Mayer, J. W., et al. "Dopant activation in ion implanted silicon by microwave annealing", Journal of Applied Physics 2009, Volume:106 Issue:11, p114902 - 114902-8.

簡介 (Vita)

姓名：謝其儒

性別：男

出生日：１９８５年１１月２７日

出生地：台灣台北市

學歷：大同大學電機工程系　學士班

　　　２００４年９月　－　２００８年６月

　　　國立交通大學電子物理研究所　碩士班

　　　２００９年９月　－　２０１１年６月

碩士論文題目：

經由微波退火形成極薄且均勻厚度的鎳矽化物研究

A study of Ultrathin and Homogenous Ni Silicide Formed by Low Temperature Microwave Annealing